Chemico-Biological Interactions 392 (2024) 110925

Contents lists available at ScienceDirect

Chemico-Biological Interactions

journal homepage: www.elsevier.com/locate/chembioint

Research paper

Assessments of carbon nanotubes toxicities in zebrafish larvae using multiple physiological and molecular endpoints

Gilbert Audira [a,b,1], Jiann-Shing Lee [c,1], Ross D. Vasquez [d,e,f], Marri Jmelou M. Roldan [g], Yu-Heng Lai [h], Chung-Der Hsiao [a,b,i,j,*]

[a] Department of Bioscience Technology, Chung Yuan Christian University, Chung-Li, 320314, Taiwan
[b] Department of Chemistry, Chung Yuan Christian University, Chung-Li, 320314, Taiwan
[c] Department of Applied Physics, National Pingtung University, Pingtung, 900391, Taiwan
[d] Department of Pharmacy, Faculty of Pharmacy, University of Santo Tomas, Manila, 1015, Philippines
[e] Research Center for the Natural and Applied Sciences, University of Santo Tomas, Manila, 1015, Philippines
[f] The Graduate School, University of Santo Tomas, Manila, 1015, Philippines
[g] Faculty of Pharmacy, The Graduate School, University of Santo Tomas, Espana Blvd., Manila, 1015, Philippines
[h] Department of Chemistry, Chinese Culture University, Taipei, 11114, Taiwan
[i] Center of Nanotechnology, Chung Yuan Christian University, Chung-Li, 320314, Taiwan
[j] Center for Aquatic Toxicology and Pharmacology, Chung Yuan Christian University, Chung-Li, 320314, Taiwan

ARTICLE INFO

Keywords:
Carbon nanotubes
Zebrafish
Larva
Embryo
Toxicity

ABSTRACT

In recent years, carbon nanotubes (CNTs) have become one of the most promising materials for the technology industry. However, due to the extensive usage of these materials, they may be released into the environment, and cause toxicities to the organism. Here, their acute toxicities in zebrafish embryos and larvae were evaluated by using various assessments that may provide us with a novel perspective on their effects on aquatic animals. Before conducting the toxicity assessments, the CNTs were characterized as multiwall carbon nanotubes (MWCNTs) functionalized with hydroxyl and carboxyl groups, which improved their solubility and dispersibility. Based on the results, abnormalities in zebrafish behaviors were observed in the exposed groups, indicated by a reduction in tail coiling frequency and alterations in the locomotion as the response toward photo and vibration stimuli that might be due to the disruption in the neuromodulatory system and the formation of reactive oxygen species (ROS) by MWCNTs. Next, based on the respiratory rate assay, exposed larvae consumed more oxygen, which may be due to the injuries in the larval gill by the MWCNTs. Finally, even though no irregularity was observed in the exposed larval cardiac rhythm, abnormalities were shown in their cardiac physiology and blood flow with significant downregulation in several cardiac development-related gene expressions. To sum up, although the following studies are necessary to understand the exact mechanism of their toxicity, the current study demonstrated the environmental implications of MWCNTs in particularly low concentrations and short-term exposure, especially to aquatic organisms.

1. Introduction

Carbon nanotubes (CNTs) are cylindrical structures comprising graphene sheets rolled in a hexagonal arrangement of sp^2 hybridized carbon atoms [1–4]. Since these rolled sheets can be single or multiple, they are categorized as single-wall carbon nanotube (SWCNTs) with a size range of 0.6–2.4 nm [4], double-wall carbon nanotube (DWCNTs) with a size range of 1–3.5 nm [5], and multiple wall carbon nanotube (MWCNTs) with a size range of 2.5–100 nm with an interlayer separation of 0.34 nm average [4]. The tubular structure of SWCNTs is available in an open or closed arrangement at both ends and hence agglomerates after sonication depicting a hydrophobic nature [6]. In comparison, DWCNTs and MWCNTs demonstrate open ends on both sides of the tubular structure, ensuring partial water solubility and minor semi-transparent dispersion [6]. CNTs are small and have good surface functionalization, high reactivity, high surface area, high

* Corresponding author. Department of Bioscience Technology, Chung Yuan Christian University, Chung-Li, 320314, Taiwan.
E-mail address: cdhsiao@cycu.edu.tw (C.-D. Hsiao).
[1] equal contribution authors.

https://doi.org/10.1016/j.cbi.2024.110925
Received 31 July 2023; Received in revised form 1 October 2023; Accepted 20 February 2024
Available online 5 March 2024

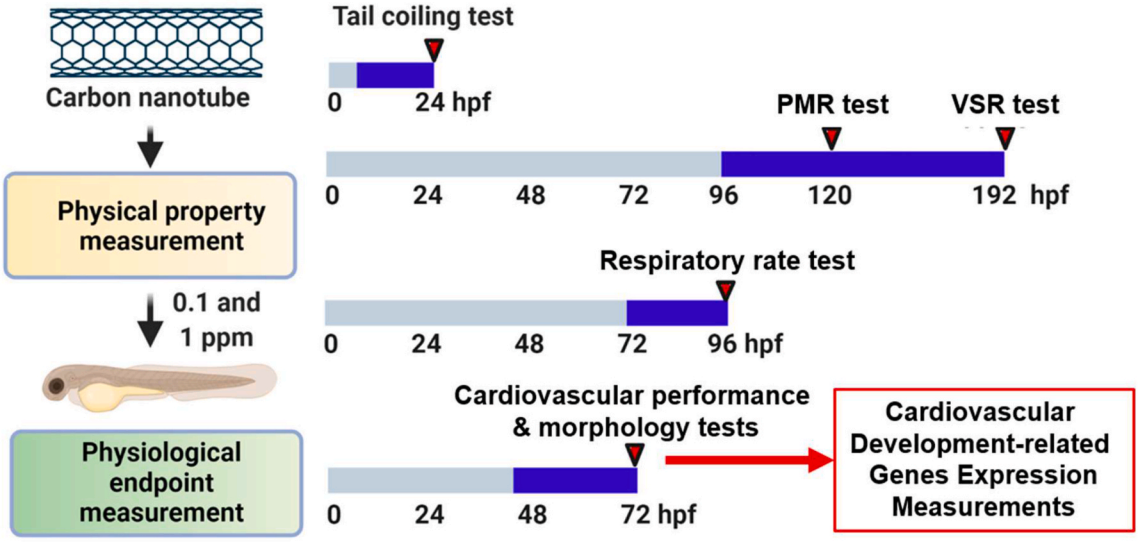

Fig. 1. Workflow overview of the current study in assessing the toxicities of carbon nanotubes on zebrafish. Right panel: Schematic for the carbon nanotubes administration exposure time for each test.

transparency, high thermal conductivity, good photoluminescence properties, and biocompatibility [3]. Owing to these properties, CNTs are actively used in the fields of electronics [7], catalysis and analysis [8,9], environmental remediation [10], energy [11], and biomedicine [12–14]. However, despite their remarkable properties and extensive scope of application, many research groups show concern for their toxicity since most CNT products are entering the aquatic environment and could profoundly influence both human and environmental health [15–17].

In an aqueous circulation, CNTs tend to spontaneously agglomerate and emerge rapidly in the shape of particulate material, making them easier to interact with cells. Even though these properties make CNTs a promising vehicle for delivery and biosensing [18], they also could lead to different toxic routes by affecting cell signaling and inducing DNA damage, membrane perturbations, and oxidative stress [19–21]. A previous study in mice reported that MWCNTs were a very important factor in cytotoxicity due to their surface hydrophilicity [22]. In addition, another finding demonstrated the toxicity of MWCNTs in common carp (*Cyprinus carpio*), which decreased its growth and survival rates with increments in blood glucose level, secretion of cortisol, and activity of anti-oxidative enzymes [23]. In addition, only a little information regarding the interaction of CNTs with the aquatic environment is available [24–30]; therefore, a validation of the CNTs' biocompatibility and safety in the aquatic environment is needed.

Recently, zebrafish (*Danio rerio*) was proposed by U.S Food and Drug Administration (FDA) as a suitable *in vivo* toxicological model for toxicity studies and drug screening for future health care assessments and treatment of diseases in humans [31] as its genome is fully

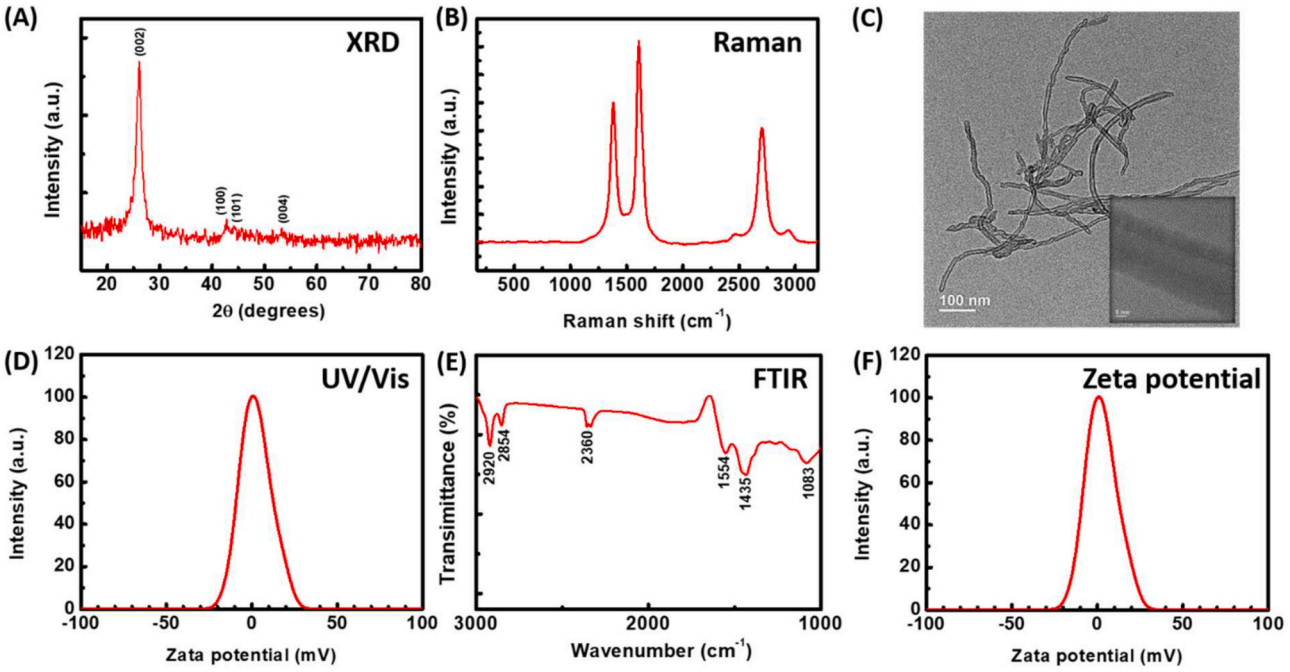

Fig. 2. Analyses of physical properties of carbon nanotubes. **(A)** XRD analysis; **(B)** Raman spectrum; **(C)** TEM observation and selected HRTEM micrograph (smaller panel); **(D)** UV–vis absorption spectrum; **(E)** FTIR spectrum; **(F)** Zeta potential measurement.

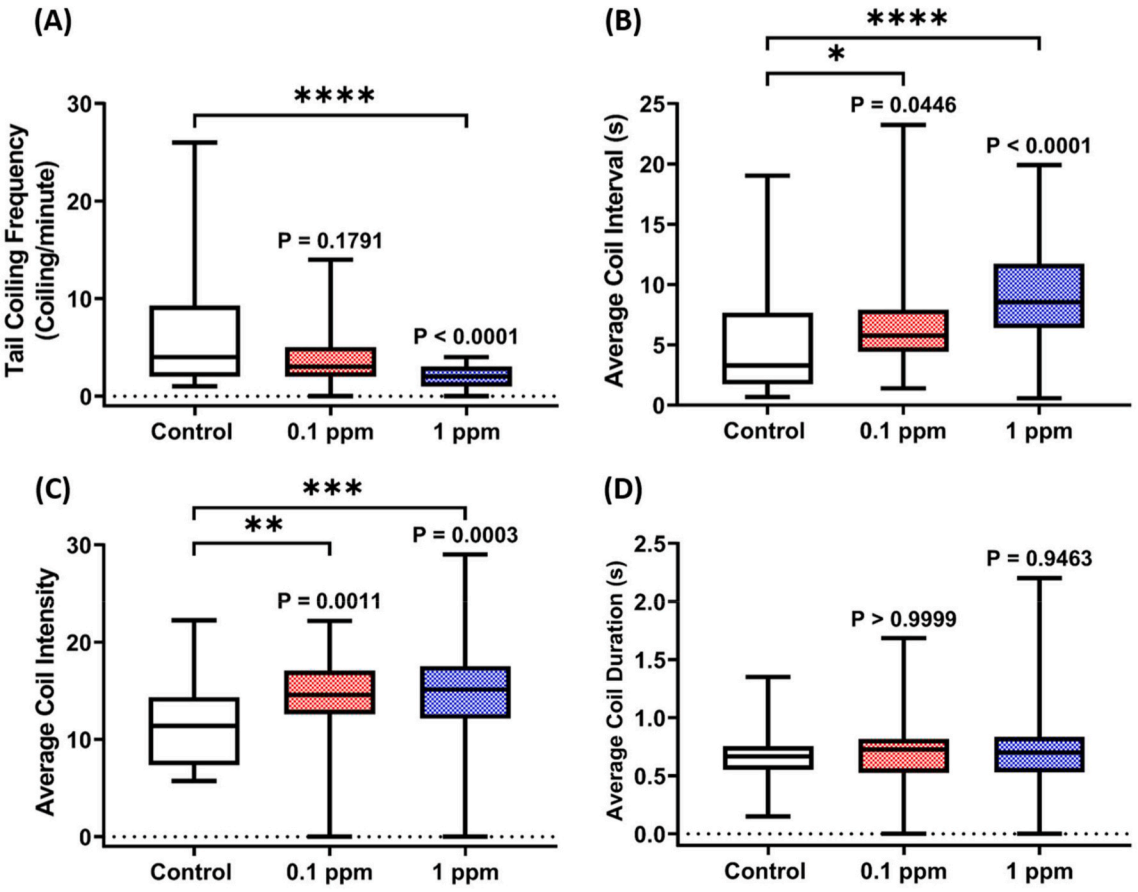

Fig. 3. Comparison of tail coiling activity of 24 hpf zebrafish embryos after exposure to 0 (control), 0.1, and 1 ppm of CNTs for 18 h. The **(A)** tail coiling frequency, **(B)** average coil interval, **(C)** average coil intensity, and **(D)** average coil duration of every fish in each group were measured. The data are presented as box and whiskers (min to max) and analyzed with Kruskal-Wallis test continued with Dunn's multiple comparisons tests ($n = 50$; $^{*}P < 0.05$, $^{**}P < 0.01$, $^{***}P < 0.001$, $^{****}P < 0.0001$).

sequenced and bears homogeneity with the human genome [32–34]. Based on phylogenetic analysis of zebrafish and the human genome, it is demonstrated that they have morphological and physiological resemblance amongst digestive, cardiovascular, and nervous systems [35]. Furthermore, the use of zebrafish in drug screening also had been cited to be consistent with the 3R concept of replacement, reduction, and refinement, where larval zebrafish demonstrates to be a critical model system for evaluating first-line screening of drugs before testing them on other model organisms [36,37]. In addition, the small size, transparency in the initial stages of growth and development, and rapid reproduction and development make zebrafish an ideal model for toxic drug screenings and studies [38].

The current research aimed to investigate the adverse effects in zebrafish embryos and larvae under acute exposure to MWCNTs at concentrations of 0.1 and 1 ppm. We hypothesized that even in relatively low concentrations, short-term exposure to MWCNTs could cause various effects in the development stages of zebrafish. Finally, the findings of this study could provide novel information regarding the MWCNTs' biocompatibility and safety in the aquatic environment. The overview of the current study design and the exposure time and period is illustrated in Fig. 1 (see Fig. 3) (see Fig. 2).

2. Materials and methods

2.1. Characterization of carbon nanotubes properties

Carbon nanotubes (2 mg/ml) as a 100 ml aqueous suspension were acquired from Tanfeng Tech. Inc. (Suzhou, Jiangsu, China). Afterward, to obtain more information regarding its bulk and surface structure, several relevant characterization techniques, which were X-ray diffraction (XRD), Raman spectroscopy, transmission electron microscopy (TEM), Fourier-transform infrared spectroscopy (FTIR), and ultraviolet–visible spectroscopy (UV–vis), were conducted.

XRD analysis was used to assess the crystallinity and interplanar distance (*d*-spacing) of the samples by observing the intensity of occurred peaks. After vacuum dried on a silicon substrate, the XRD patterns of the samples were analyzed by using Bruker D8 Advanced eco (Billerica, MA, USA) with a CuKα radiation source. An angular range of 15°-80° (2Θ), a 0.02° step size, and 2s per step was used as the scanning condition. The voltage for the X-ray tube was adjusted at 40 kV while its current was set at 30 mA. For Raman spectroscopy analysis, the excitation wavelength of 532 nm was used and the range of the scanned spectral was 180–3200 cm^{-1} with a resolution of 1 cm^{-1}. The exposure time was 5 s with a total of 5 scans per spectrum. This analysis was conducted using a microscopic Raman system (RAMaker, Protrustech Co., Ltd., Taiwan). A small quantity of the samples was dipped on a glass substrate. After the air-drying process, their Raman spectrum was collected under a 20 × objective lens and their size, shape, and surface morphology were observed by using the images captured by JEOL (JEM-2100 F/Cs) high-resolution transmission electron microscope (HRTEM). Meanwhile, for TEM analysis, about 0.1 ml of diluted dispersion was used and dropped on Cu grids coated with a carbon film. Next, in the UV–vis analysis, a Jasco V-770 double beam spectrophotometer (Jasco Co., Japan) was utilized to automatically monitor the light absorbance of these materials from 200 to 800 nm. Meanwhile, a Jasco FTIR-6700 spectrometer in transmission mode was used to record the FTIR

spectrum in the range of 3000 to 1000 cm^{-1}. The measurements were conducted with MWCNTs that had already been mixed with KBr and pressed into a pellet. Finally, the zeta potential of the samples was also measured to evaluate their colloidal dispersions' stability. Prior to the measurement, the samples were homogenized for 15 min by high-intensity ultrasonic waves. Subsequently, the electrical potential was measured at 25 °C by an SZ-100 dynamic light scattering system (Horiba, Kyoto, Japan).

2.2. Zebrafish maintenance

The AB zebrafish originated from Taiwan Zebrafish Stock Center at Academia Sinica (TZCAS) and was used for breeding. The adult zebrafish were reared in a continuous aerated water system at 26 ± 1 °C with 14/10 h of light/dark cycle. The protocol for animal housing was based on the prior publication [39]. For the breeding process, one female and two male adult zebrafish were used with the help of a breeding chamber. After the mating process, the eggs were collected and incubated at 28 ± 1 °C in distilled water mixed with methylene blue (0.0001%) as a fungicide until the exposure was started. Healthy embryos and larvae without any signs of infection were selected and used. The experiment was carried out correspondingly to the guidelines for the care and use of Laboratory Animals by Chung Yuan Christian University (CYCU) and authorized by the Animal Ethics Committee of CYCU with the ethical approval number CYCU110016.

2.3. Carbon nanotubes exposure

Carbon nanotubes from the stock solutions were diluted with double distilled water until the concentrations of 0.1 and 1 ppm working solution were reached. Although these concentrations are higher than the predicted environmental concentration in water (1×10^{-9} to 5×10^{-7} ppm) [28,29], these are relatively lower than the concentrations used in earlier studies of CNTs in various animal and other models, such as mice (25–10,000 ppm) [40–42], green algae (1.8–40 ppm) [30], *Oryzias latipes* (100 ppm) [27], and adult (2 ppm) [43] and larval zebrafish (0.08–22,050 ppm) [24–26,44,45]. In addition, low concentrations of CNTs were chosen considering their higher sensitivity and informativeness than other toxicological and pharmacological assessments. Therefore, the relatively low concentrations that were applied in the present study might reveal novel toxicity properties of MWCNTs. In improving the dispersion of nanoparticles, the solutions were sonicated prior to the exposure [46]. For the tail coiling assay, 6 hpf zebrafish embryos were exposed for 18 h. Meanwhile, for the photomotor response and vibrational startle response assays (VSRA), the MWCNTs were administered to 96 hpf zebrafish larvae for 24 (photomotor response) and 96 h (VSRA). Next, before the oxygen consumption test, 72 hpf zebrafish larvae were exposed to MWCNTs for 24 h while for the cardiovascular performance assay and morphology observation, the incubation was conducted on 48 hpf zebrafish larvae for 24 h. The incubation period for each test is illustrated in Fig. 1. Trained observers blinded to the treatments were chosen to conduct all of the tests.

2.4. Tail coiling assessment in zebrafish embryos

After 18 h of exposure to MWCNTs, zebrafish embryos were placed in 1% agarose wells prepared in a Petri dish. Later, in the 28 ± 1 °C incubator, a charge-coupled device (CCD) camera (Zgenebio, Taipei, Taiwan) was installed on a dissecting microscope (Shenzhen Saike Digital Technology Development Co., Ltd., Shenzhen, China) was used to record the tail coiling activity of each embryo for 1 min with 30 fps with 1920 × 1080 pixels of resolution videos. By using VirtualDub2 software (http://virtualdub2.com/), the video format was converted from. mp4 format to. avi format. Next, to gather and analyze the obtained data based on the videos, ImageJ FIJI builds (https://imagej.net/Fiji/Downloads) and Microsoft Excel 2016 were used. Several tools and plugins were downloaded and installed before the data extraction process. Afterward, the StackDifference plugin was used to generate a subtracted image stack that will show the difference between video frames. Later, the Plot Z-axis Profile tool and BAR Plugin were utilized to extract the tail coiling occurrence. Finally, the results were saved as an Excel (.xlsx) file to calculate several important endpoints, including tail coiling frequency, average coil interval, average coil intensity, and average coil duration. A more detailed explanation of this protocol and the scripts used during the data extraction process can be found in the previous publication [47]. Following previous publications, this assay was conducted in two replicates with a total *n* number of 50 embryos in each group [48,49]. In addition, this sample size was chosen based on the results of statistical power analysis in the control group that showed a 99.99% confidence interval (CI) and a margin of error of 2 units if this sample size was applied [50].

2.5. Photomotor response assessment in zebrafish larvae

The photomotor response of zebrafish larvae was assessed after 24 h of exposure to MWCNTs. The 48-well transparent plastic plate with the tested zebrafish larvae in each well was put into Zebrabox (Viewpoint, Civrieux, France). Afterward, the locomotion of tested larvae was recorded and measured by ViewPoint system, a video tracking software (Viewpoint, Civrieux, France). Prior to the photomotor response test, the larvae were habituated in the chamber for ~30 min without any stimulus. After habituation, the test was started with 80 min of video recording, which consisted of four 20-min cycles that consisted of each 10-min light and dark period. The tracking process interval was set to 1 min, thus, generating 80 data points. In addition, a larval photomotor response (LPMR) was also calculated to measure the swimming responses of the larvae to a sudden change in light conditions. LPMR for each photoperiod transition was calculated as the differences between the mean of distance traveled in the first time point of a certain period with the mean in the last time point of its previous period. All settings used in the protocol were based on previous publications [51,52]. This test was done in triplicate with a total sample size of 94 ± 1 for each group. The *n* number determination was based on a prior experiment, and statistical power analysis in the control group with a CI of 98% with 4 margins of error that suggested a sample size of 83 was required [50,53].

2.6. Vibrational startle response assay in zebrafish larvae

After zebrafish larvae were exposed to MWCNTs for 96 h, a vibrational startle response assay was conducted on 8 days post-fertilization (dpf) larvae. Similar to the photomotor response assessment, Zebrabox and ViewPoint systems (Viewpoint, Civrieux, France) were used to measure the locomotion of zebrafish larvae in every well of the 48-well plate. After 30 min of habituation, the test was started with the first 5 s without any stimulus followed by 20 s of tapping stimulus with a 1-s interstimulus interval (ISI). The intensity level of the tapping stimulus was set at 100%. Each larva's vibrational startle response was analyzed by measuring its distance traveled every second after the stimulus was given. The current procedure was based on the prior study [54]. This assessment was carried out in two replicates with a total sample size of 68, 75, and 70 for control, 0.1, and 1 ppm groups, respectively. The sample size determination was based on earlier publications [54,55], and this *n* number was selected based on statistical power analysis in the control group that suggested the use of at least 42 larvae in order to reach 99.9% CI with 1 unit of margin of error [50]. The mortality of the fish caused the slight differences in *n* number between each group during the incubation for unknown reasons, which might be related to the longer incubation periods compared to other tests.

2.7. Respiratory rate assay in zebrafish larvae

The oxygen consumption rate assay was conducted on 96 hpf zebrafish larvae after 24 h of incubation of MWCNTs by using a Microplate system by Loligo Systems (Loligo Systems, Viborg, Denmark). Each well with a tested larva of a 24-well plate with the Sensor Dish Reader (SDR) below it was filled with 80 μL of the compound. One well was kept empty to be used as a blank. Later, MicroResp™ software version 1.0.4 (Loligo Systems, Viborg, Denmark) was executed to measure the oxygen consumption every minute in each well for 80 min. The protocol was conducted based on several prior publications [56,57]. This assay was conducted in two replicates with a total sample size of 46 larvae for each group. In addition to a prior study, this *n* number was determined by a statistical power analysis conducted in the control group, which showed that 42 samples were needed to obtain the results with 99.9% CI with 0.5 units of margin of error [50,58].

2.8. Zebrafish larval cardiovascular performance assay

Zebrafish embryos at 72 hpf exposed to MWCNTs for ~24 h were used in this assessment. Zebrafish larvae were transferred to a plastic dish, and to reduce the larval movement during the recording process, 3% methylcellulose was added. For the heartbeat and blood flow recording process, a high-speed digital CCD (AZ Instruments, Taichung, Taiwan) was mounted on an inverted microscope (ICX41, Sunny Optical Technology, Yuyao, China) was used to obtain a video with 200 frames per second (fps). Here, two lenses, which were LPlans objective lens with 10 × magnification and Hoffman objective lenses with 40 × magnification, were utilized to examine the rhythm of the heart chamber and observe the cardiac physiology that primarily focused on the ventricle position and blood vessel in the dorsal aorta (DA), respectively. The video was recorded for 10 s using HiBest Viewer software (AZ Instrument, Taichung, Taiwan). The rhythm of the heart chamber was measured by using the Time Series Analyzer plugin on ImageJ Software version 1.53c (https://imagej.nih.gov/ij/plugins/time-series.html). Furthermore, sd1 and sd2 of both heart chambers were calculated using the Poincare plot plugin from Origin Pro 2019 software (OriginLab Corporation, Northampton, MA, USA) in order to evaluate the variability of their heartbeat. In addition, some cardiac physiology endpoints such as stroke volume, cardiac output, and ejection and shortening fractions, were also evaluated. Stroke volume shows blood volume that is ejected from the heart chamber with each contraction, while cardiac output is the amount of blood a heart pumps from the ventricle per minute. With measuring the amount of pumped blood out of the ventricle, which also refers to the ability of the heart to pump blood, ejection fraction was calculated, which is correlated with shortening fraction as it calculates the changing percentage in the dimension of the ventricle during the systolic phase [59]. For the blood flow measurement, the position of blood cells in every frame was obtained by using 'Trackmate" plugin on ImageJ. Later, the output results were analyzed using Microsoft Excel to obtain the speed value of the detected blood cells. All protocols used in this assay were according to the prior studies [60–62]. In obtaining the blood flow profile, a file consisting of two rows of data (time and blood flow speed per frame for each detected blood cell) was smoothed using the smooth function from Origin Pro 2019. Later, the results were copied to GraphPad Prism (GraphPad Software version 8 Inc., La Jolla, CA, USA) (https://www.graphpad.com/) to output as a graph. Three replications with a total *n* number of 30 larvae for each group were applied in the current test. The *n* number was determined from several prior studies, and a statistical power analysis conducted in the control group showed a CI of 90–95% with 3–11 units of margin error [50,63,64]. In addition, the changes in their morphology were evaluated by measuring their body length and eye axis length, together with the quantifications of their pericardial cavity area by using ImageJ software.

2.9. Gene expression analysis

Based on the alterations in cardiac physiology and blood flow led by MWCNTs, the gene expression related to the induction of cardiac development was assessed. The incubation was repeated as a cardiovascular performance assay. Afterward, the total RNA of each group that consisting of 60–70 larvae was isolated using RNAzol reagent (Molecular Research Center, Inc., Cincinnati, Ohio, US). The quality of RNA was assessed by UV spectrophotometry and the total RNA was reversed to cDNA by using SuperScript II transcriptase (18,064–014, Thermo Fisher Scientific, MA., USA). All primers were designed by Integrated DNA Technologist (IA, USA) and their sequences are shown in Table S1. Real-time PCR system StepOne™ System (Thermo Fisher Scientific, MA., USA) was used to perform the quantitative real-time PCR (qRT-PCR) amplifications with beta-actin as a control with the following parameters: denaturation for 0 s at 95 °C, followed by 30 cycles at 95 °C for 3 s and 58 °C for 30 s. During the annealing/extension step, the occurred fluorescent signal was measured. In addition, melt curve analyses were also performed to assess qPCR amplicon length. Since the transcription of *β-actin* was considered as an internal control, the relative expression level of each mRNA was calculated using the $2^{-\Delta\ \Delta}$Ct method and expressed in accordance with its ratio to *β-actin* mRNA [65,66]. Three biological replicates were performed per group and all of the experiments were carried out according to the manufacturer's protocol.

2.10. Statistical analysis

All of the statistical analyses were carried out using GraphPad Prism. Before statistical comparison analysis was conducted, D'Agostino-Pearson, Anderson-Darling, and Shapiro-Wilk tests were performed to evaluate the data distribution normality. The data that did not pass those normality tests were analyzed by Kruskal-Wallis test followed by Dunn's test, non-parametric analyses, since the assumption of normally distributed data is not required by these tests [67]. On the other hand, if the data passed the normality tests, the statistical differences between each treated group and control group were analyzed using one-way ANOVA, followed by Dunnett's multiple comparisons test. Meanwhile, a two-way ANOVA test with Geisser-Greenhouse correction followed by Dunnett's multiple comparisons test was used for the chronology data. The statistical differences were marked either by asterisks of "*" ($P < 0.05$), "**" ($P < 0.01$), "***" ($P < 0.001$), or "****" ($P < 0.0001$).

3. Results and discussion

3.1. Analysis of physical property of carbon nanotubes

Although CNTs are considered non-crystallized material, their structure demonstrated distinct X-ray diffraction peaks [68]. Fig. 1A illustrates a characteristic diffraction peak of (002) at 26.1° with high intensity, suggesting that the graphitic structure was preserved [69]. This value was calculated as an average distance between graphene layers (d_{002}) using Bragg's Law, which is 0.34 nm. Moreover, the appearance of three weak peaks around $2\theta = 42.8°$, 44.2°, and 53.3° was attributed to the diffraction of the (100), (101), and (004) crystallographic planes, respectively [70,71].

Next, Raman spectroscopy, a particularly well-suited technique to characterize the molecular morphology of carbon materials and assist in distinguishing the presence of CNTs relative to other carbon allotropes, was carried out. Three characteristic peaks were observed for the test sample: D-band at 1325 cm^{-1}, G-band at 1576 cm^{-1}, and G′- band at 2647 cm^{-1} (Fig. 1B). The complete disappearance of the RBM mode and small I_D/I_G ratio confirmed that the CNTs used in this study belong to MWCNTs.

Afterward, the outer diameter distributions of the tubular nanostructures were estimated using HRTEM, a technique to determine how the tubular nanostructures are arranged, as seen in Fig. 1C. Accordingly,

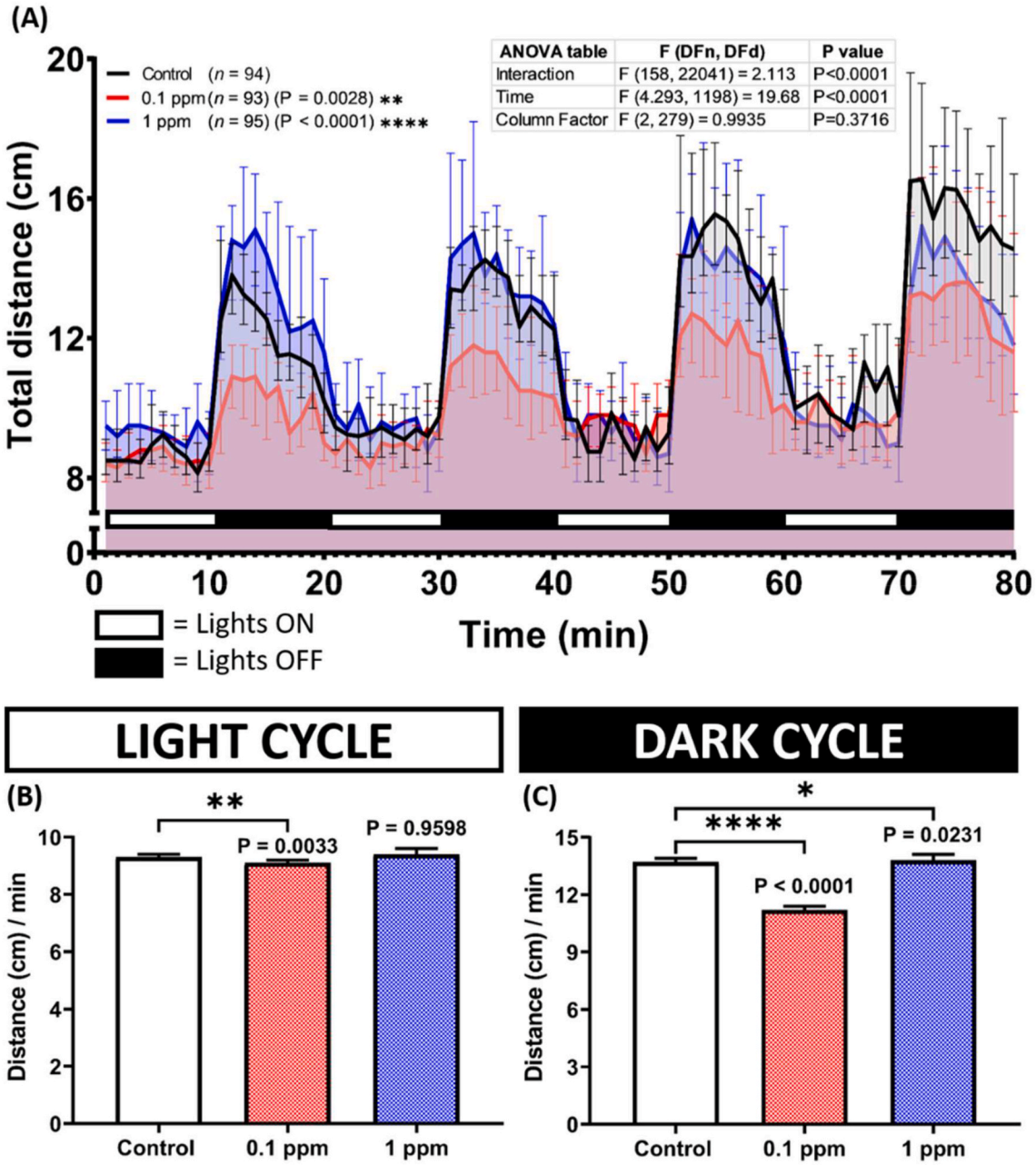

Fig. 4. **(A)** Total distance traveled per minute by 128 hpf zebrafish larvae after 1-day exposure of 0 (control), 0.1 ppm, and 1 ppm of carbon nanotubes during both light and dark cycles. The data were analyzed by using a two-way ANOVA test with Geisser-Greenhouse correction, followed by Dunnett's multiple comparisons test. **(B–C)** Comparison of total distance traveled by the tested zebrafish larvae in light and dark cycles, respectively. The data were analyzed using Kruskal-Wallis test, continued with Dunn's multiple comparisons test. All data are expressed in median with 95% CI ($n = 94$ for control, $n = 93$ for 0.1 ppm, $n = 95$ for 1 ppm; *P < 0.05, **P < 0.01, ****P < 0.0001).

the mean outer diameter of the examined MWCNTs sample is estimated to be 19.7 nm. In addition, the HRTEM image of these nanotubes at higher magnification displays clear lattice fringes with fine parallel lines along the tube axis, indicating a crystalline graphene layers structure (Fig. 1C). The mean distance between adjacent graphene layers in MWNTs is 0.35 nm, which is close to the d_{002} value.

Further, plasmon resonance, a joint density of states for a simple graphene layer, can be investigated in the UV range [72]. An absorption maximum is generally observable in the UV range of the spectrum (206.1 and 251.2 nm (6.02–4.94 eV)) for all nanotubes [73]. To minimize the effect of surfactants or polymers that are generally utilized for the solubilization of MWCNTs, a thorough rinse of the test sample has been performed to ensure that the spectroscopic features observed in our experiments belong to nanotubes. As in the case of the MWCNTs suspension, a characteristic absorption band at 260 nm was recorded, in which the absorption maximum slightly shifted to a longer wavelength (Fig. 1D). FTIR is commonly employed to investigate functionalization. In Fig. 1E–six absorption bands at ~2920, ~2854, ~2360, ~1554, ~1435, and ~1083 cm^{-1} were observed. Lastly, zeta potential is the potential difference existing between colloidal particles. Our measurements show that the mean value of the MWCNTs suspension is −0.1 mV (Fig. 1F).

3.2. The effects of MWCNTs on tail coiling of zebrafish embryos

First, the potency of MWCNTs in affecting the larval tail coiling (TC)

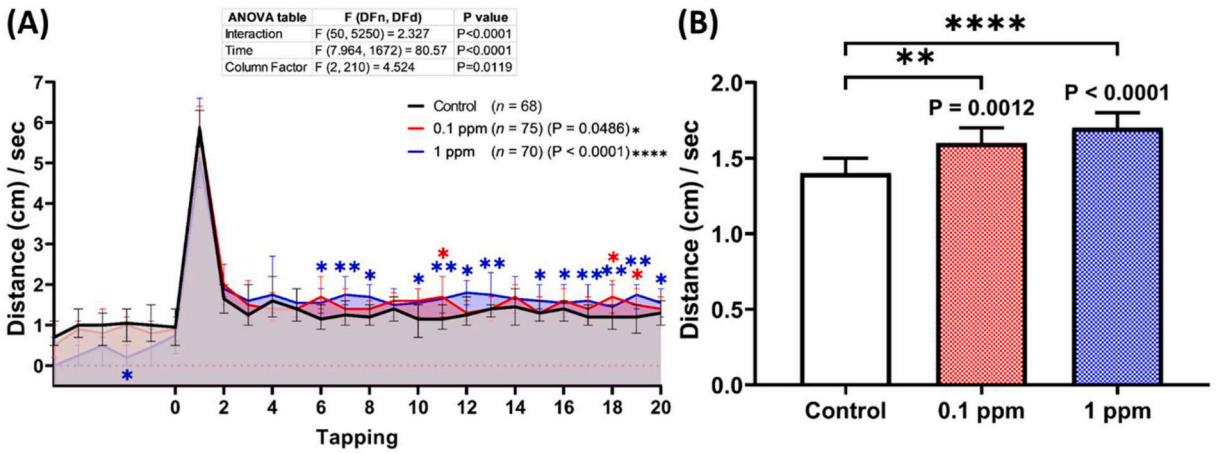

Fig. 5. **(A)** Total distance traveled per second by 192 hpf zebrafish larvae after 4-days exposure of 0 (control), 0.1 ppm, and 1 ppm of carbon nanotubes during the vibrational startle response assay. The data were analyzed using a two-way ANOVA test with Geisser-Greenhouse correction, followed by Dunnett's multiple comparisons test. **(B)** Comparison of the total distance traveled by the tested zebrafish larvae during the tapping stimuli occurred. The data were analyzed using the Kruskal-Wallis test, continued with Dunn's multiple comparisons test. All data are expressed in median with 95% CI ($n = 68$ for control, $n = 75$ for 0.1 ppm, $n = 70$ for 1 ppm; *P < 0.05, **P < 0.01, ****P < 0.0001).

behavior as the first locomotor activity of zebrafish embryos was evaluated [44,45,48]. Here, the tail-coiling behaviors of each group were monitored after 18 h of exposure to MWCNTs. A statistical reduction in tail coiling frequency was observed in the 1 ppm-treated group (Fig. 1A). Furthermore, all the exposed groups had their average coil interval, and average coil intensity increased, indicating a less frequent but more robust TC (Fig. 1B&C). However, both treated groups did not show any statistical differences from the control group in terms of average coil duration (Fig. 1D). Taken together, acute exposure to MWCNTs in low concentration altered the tail-coiling behavior in zebrafish embryos.

3.3. The effects of MWCNTs on the photomotor response of zebrafish larvae

Next, the larval locomotion after MWCNTs exposure to light changes as the photomotor response was assessed. Based on the overall results, all exposed groups displayed a statistically different locomotion pattern during the test than the untreated group (Fig. 4A). From a detailed analysis, a low concentration of MWCNTs was found to cause a hypoactivity-like behavior during both light and dark cycles (Fig. 4B and C). Interestingly, higher locomotor activity than the control group was displayed by zebrafish larvae after being exposed to 1 ppm of MWCNTs. However, this phenomenon only occurred during the dark cycle of the test (Fig. 4C). Nevertheless, no statistical differences in the LPMR results indicated that the exposed zebrafish larvae exhibited similar swimming responses toward an abrupt shift in light conditions (Fig. S1).

3.4. The effects of MWCNTs on vibrational startle response of zebrafish larvae

A vibrational startle response assay (VSRA) was conducted to evaluate whether MWCNTs also could impair the vibrational startle response of larval zebrafish by calculating their movement distance as the response toward repetitive vibrational stimuli generated by a tapping device. From the results, MWCNTs in both concentrations statistically altered the habituation of vibrational startle response, which was shown by the increment in the area under curve (AUC) values observed in the exposed groups compared to the control (Fig. 5A). After further investigation, the alterations were verified by the statistically higher distance traveled during the occurrence of tapping stimuli by both treated groups

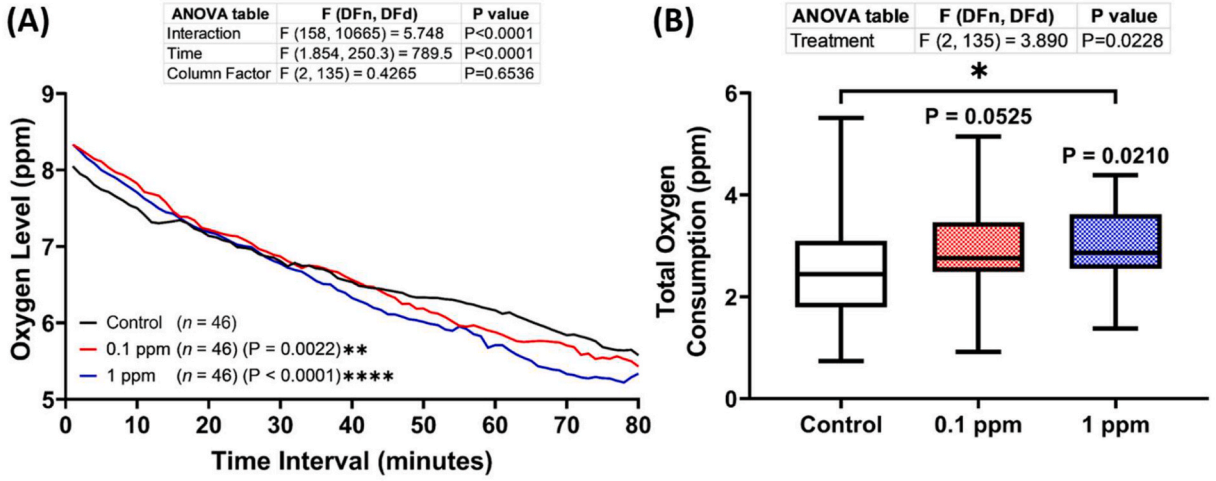

Fig. 6. **(A)** Oxygen consumption level per minute by 96 hpf zebrafish larvae after 1-day exposure of 0 (control), 0.1 ppm, and 1 ppm of carbon nanotubes during the respiratory rate assay. The data were analyzed using a two-way ANOVA test with Geisser-Greenhouse correction, followed by Dunnett's multiple comparisons test, and expressed in the median with 95% CI. **(B)** Comparison of total oxygen consumption of the tested zebrafish larvae. The data were analyzed by using one-way ANOVA, continued with Dunnett's multiple comparisons test and are presented as box and whiskers (min to max) ($n = 46$; *P < 0.05, **P < 0.01, ****P < 0.0001).

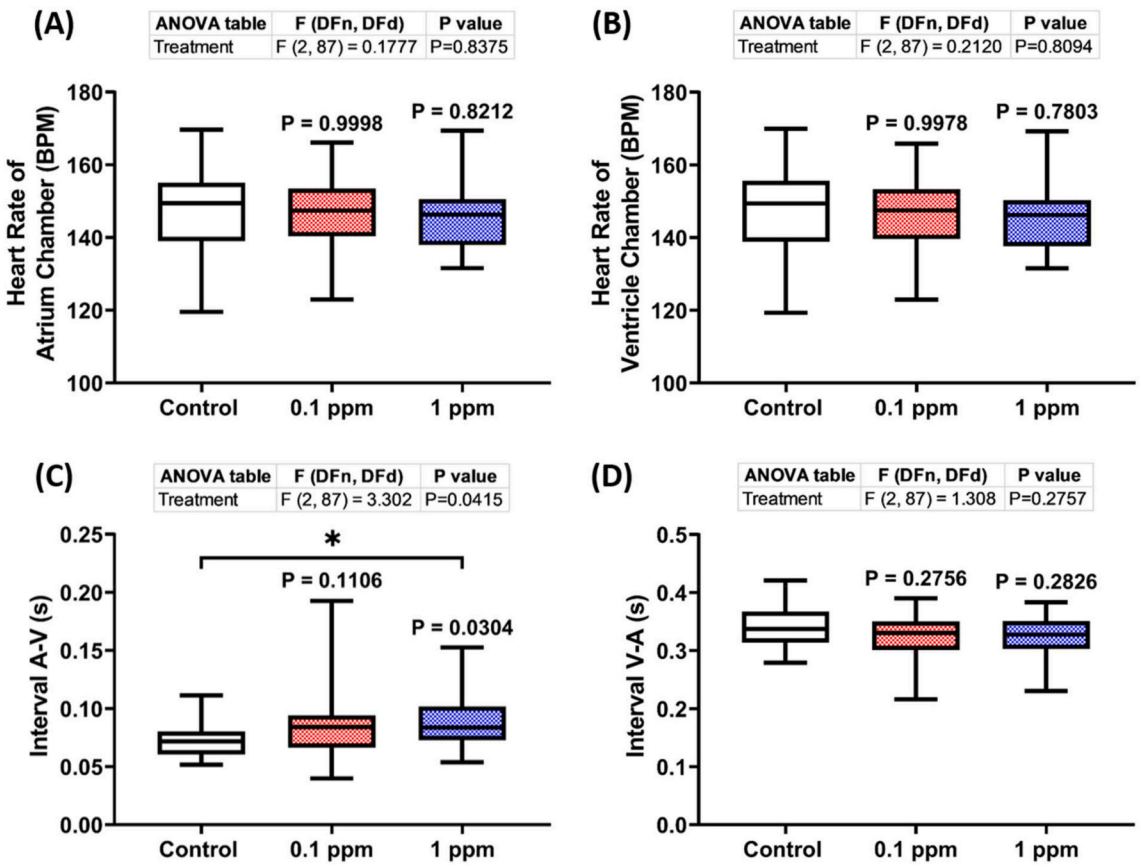

Fig. 7. Comparison of several cardiac rhythm endpoints, including heart rate of **(A)** atrium and **(B)** ventricle chamber and interval of **(C)** A-V and **(D)** (V–A) in zebrafish larvae after exposure of 0 (control), 0.1 ppm, and 1 ppm of carbon nanotubes. The data were analyzed using one-way ANOVA test, followed with Dunnett's multiple comparisons tests, and are presented as box and whiskers (min to max) ($n = 30$; *P < 0.05).

compared to the untreated group (Fig. 5B).

3.5. The effects of MWCNTs on the respiratory rate of zebrafish larvae

Numerous studies have demonstrated the respiratory and inhalation toxicity of airborne MWCNTs, therefore the respiratory effect of the current MWCNTs on zebrafish larvae was investigated in the present study [16,74–76]. After monitoring the oxygen consumption of zebrafish larvae over time, both exposed groups were found to exhibit a statistically different respiratory rate than the untreated group, as shown in Fig. 6A. Furthermore, based on the total oxygen consumption during the test, the 1 ppm-treated group was found to consume a statistically high oxygen level compared to the untreated group (Fig. 6B). Taken together, these results indicated that aqueous MWCNTs caused respiratory toxicity toward zebrafish larvae.

3.6. The effects of MWCNTs on the cardiac rhythm of zebrafish larvae

Next, the cardiotoxicity of MWCNTs was analyzed by heart rate through the ventral aorta posterior cardinal vein channel measurement. The results showed that the low-concentration-treated larvae displayed comparable heart rate and intervals in the atrium and ventricle to the untreated group (Fig. 7A–D). Interestingly, while the high-concentration-treated group also exhibited similar heart rate values, a slight increment in the interval of atrium-ventricle was observed even though their interval of ventricle-atrium was not statistically distinct from the control group (Fig. 7A–D). Remarkably, the SD1 and SD2 values of both the atrium and ventricle chambers were not changed, highlighting the regularity of the atrium and chamber beats (Figs. S2A–D). These results indicated that MWCNTs at the given concentration and exposure time did not significantly alter the zebrafish larval heart rate.

3.7. The effects of MWCNTs on the cardiac physiology of zebrafish larvae

Since there were no significant alterations in zebrafish larval heart rate after being exposed to MWCNTs, a deeper investigation of the cardiotoxicity of this compound was conducted by assessing the cardiac physiology of the larvae. Compared to the control group, both exposed groups showed decrements in most of the endpoints, including stroke volume, cardiac output, and ejection fraction (Fig. 8A–C). Interestingly, while a low concentration of CWMNTs caused a decrease in the shortening fraction, this abnormality was not found in the high-dose group (Fig. 8D). Overall, these results denoted the potential cardiotoxicity of this compound, especially in terms of cardiac physiology.

3.8. The effects of MWCNTs on the blood flow of zebrafish larvae

Since alterations in the treated larval cardiac physiology were observed in the previous test, it is intriguing to examine their blood flow since it is tightly associated with heart rate. Based on the results, the low-concentration-treated group exhibited slower blood flow than the control group. This alteration was indicated by the statistically lower average and maximum blood flow speed of this group compared to the untreated group (Fig. 9A–D). Interestingly, this effect was not shown in the high-dose group since this group showed comparable levels of both endpoints to the control group (Fig. 9A–C, E). Taken together, the results suggested that a low concentration of MWCNTs decreased the blood flow speed in zebrafish larvae without altering their cardiac rhythm.

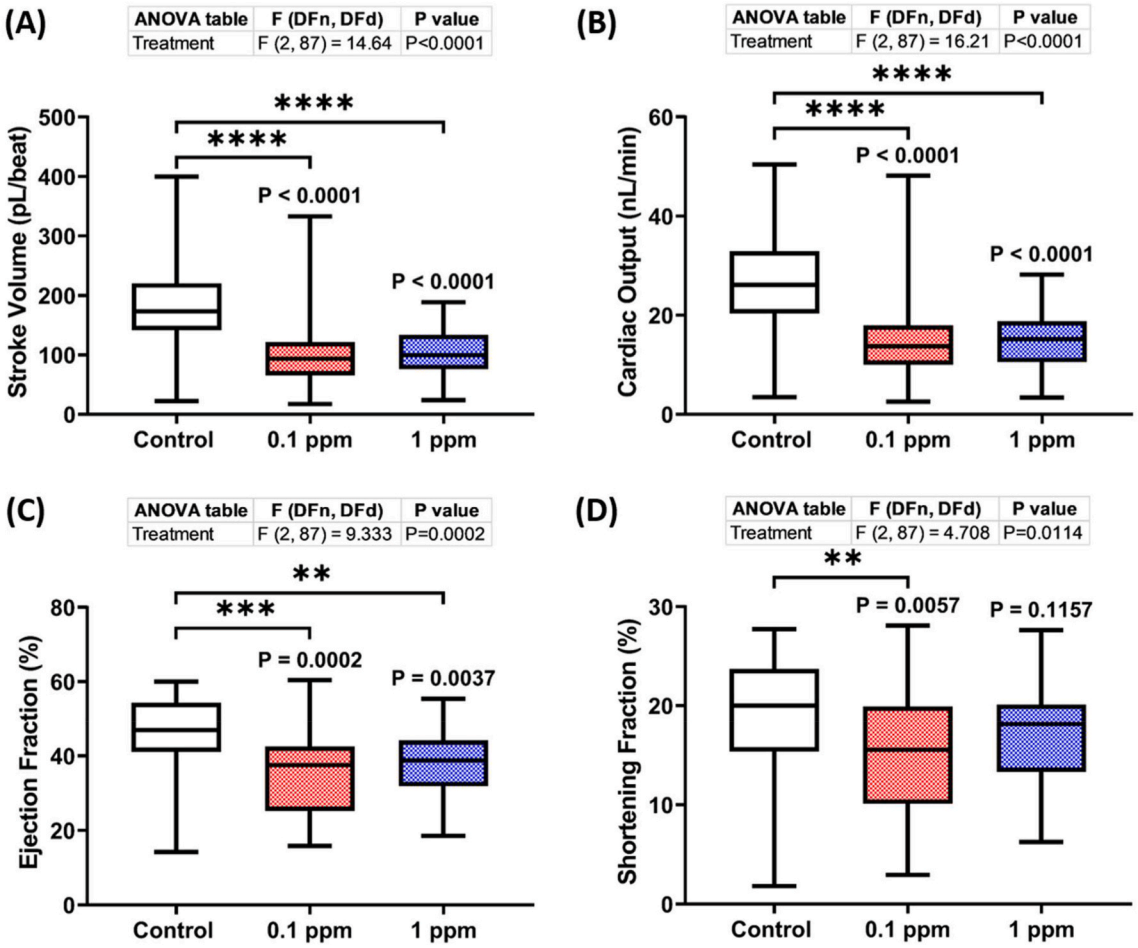

Fig. 8. Comparison of several cardiac physiology endpoints, including **(A)** stroke volume, **(B)** cardiac output, **(C)** ejection fraction, and **(D)** shortening fraction in zebrafish larvae after exposure of 0 (control), 0.1 ppm, and 1 ppm of carbon nanotubes. The data were analyzed by using one-way ANOVA test, followed with Dunnett's multiple comparisons test, and are presented as box and whiskers (min to max) ($n = 30$; **P < 0.01, ***P < 0.001, ****P < 0.0001).

3.9. Cardiovascular development-related gene expression

Although there was no abnormality observed in the cardiac rhythm, alterations were shown in their cardiac physiology and blood flow, thus; it is intriguing to evaluate the expression level of several heart marker genes by using qRT-PCR. The qRT-PCR results demonstrated that compared with the untreated group, the expression of *myh6*, a myocardia marker gene, in the low-concentration-treated group was statistically lower (Fig. 10A). Next, while both treated groups displayed no statistical difference from the control, a difference was found between each treated group in some marker genes, which were *txb5*, *nxk2.5*, *amhc*, and *gata4* (Fig. 10B–E). Finally, overall reductions in the expression level of *hbae1*, one of the embryonic globin genes, were also observed in the treated groups (Fig. 10F). Meanwhile, there was no difference in the expression level of other tested cardiovascular development-related genes, which were *vmhc*, *vegfaa*, *hbbe1*, *hbbe2*, *gata1*, *fli1*, and *vegfab*, between each group (Fig. S3). Nevertheless, acute exposure to MWCNTs in relatively low concentrations could alter several cardiovascular development-related genes in zebrafish larvae.

4. Discussion

In the present study, the toxicity of MWCNTs in the early stages of zebrafish development was investigated. Despite the numerous studies that have demonstrated the chronic toxicities of MWCNTs in aquatic organisms (Table S2), to the best of our knowledge, this is the first research that assessed the adverse effects of relatively low concentrations of this type of CNTs on the behaviors, respiratory rate, and cardiovascular performance of zebrafish larvae after acute administration. Normal morphology of embryos was observed on 72 hpf larvae, specifically in terms of their body length and eye axis length after they were exposed to MWCNTs for 24 h (Figs. S4A–E). This result is in agreement with earlier works, which did not find an alteration in zebrafish embryo development in concentrations up to 50 ppm [77]. However, several abnormalities in behaviors, respiratory rate, and cardiovascular performance were observed in the treated fish.

Prior to the biotoxic effects of CNTs, it is important to characterize the materials first. This process is necessary since a prior study showed that the formation of the large agglomerated is related to the reduction in effects of carboxyl-functionalization in their bioactivity [78]. Thus, the inconsistencies in the toxicities of functionalized MWCNTs have been attributed to the differences in their physicochemical properties [79]. From the results, the XRD pattern of the analyzed CNTs sample exhibited some distinct similarities to those of graphite powder [80], which might be due to their similarity with intrinsic graphene properties [81]. The positions of all these detected peaks are in good agreement with the results reported in the literature [70,82]. Next, based on the Raman spectroscopy results, three characteristic peaks were shown, similar to those of CNTs [71,83,84]. The D band is associated with disorder (sp^3) carbons and the G band with the crystalline graphite structures (sp^2 carbons) of CNTs [81]. The intensity ratio of these two bands (I_D/I_G) can represent the quality of graphene-based products. Although MWCNTs have very similar spectra to those of SWCNTs, the major differences are the lack of the radical breathing mode (RBM) and

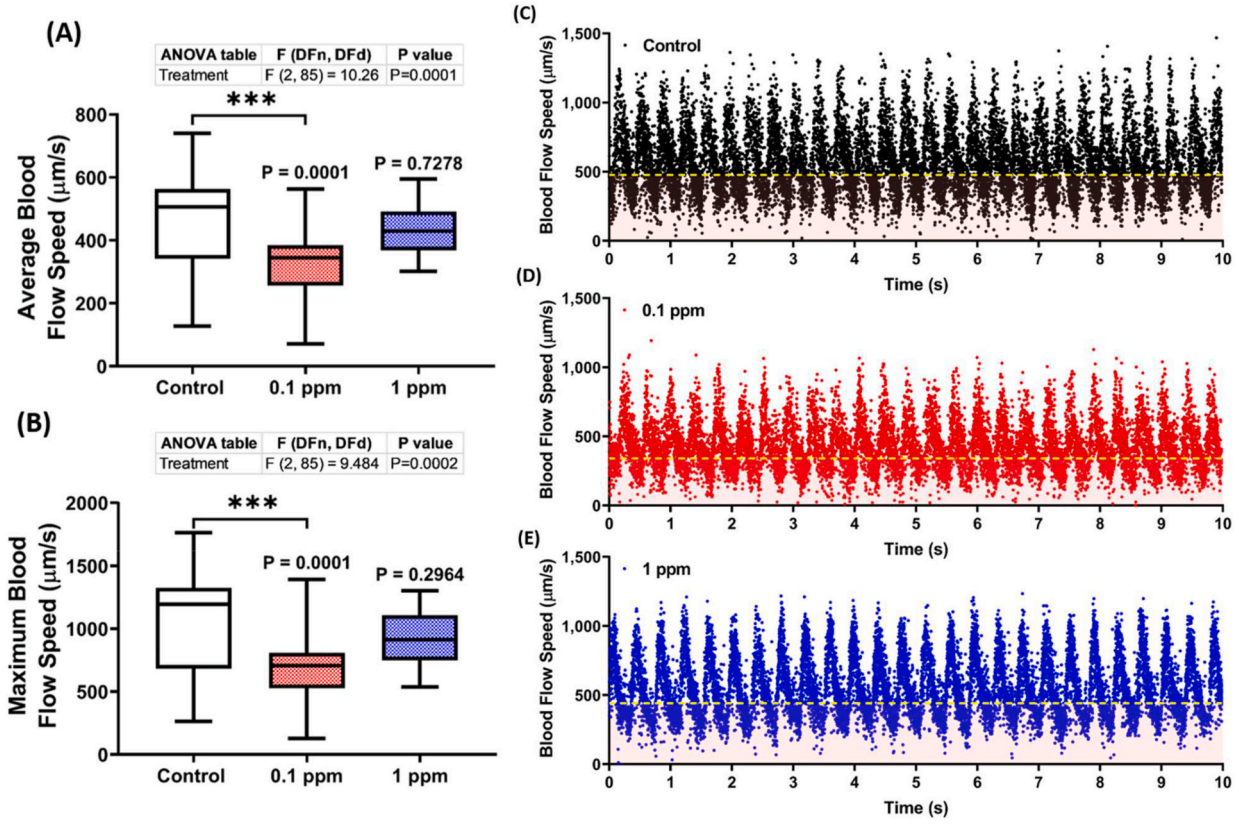

Fig. 9. Comparison of **(A)** average and **(B)** maximum blood flow speed in zebrafish larvae after exposure of 0 (control), 0.1 ppm, and 1 ppm of carbon nanotubes. The data were analyzed by using One-Way ANOVA test, followed with Dunnett's multiple comparisons test, and are presented as box and whiskers (min to max) ($n = 30$, except for 0.1 ppm group ($n = 28$); ***$P < 0.001$). The time chronology of blood flow rate speed monitored in the dorsal aorta of a single representative zebrafish larva each from **(C)** 0 (control), **(D)** 0.1 ppm, and **(E)** 1 ppm of carbon nanotubes-treated groups.

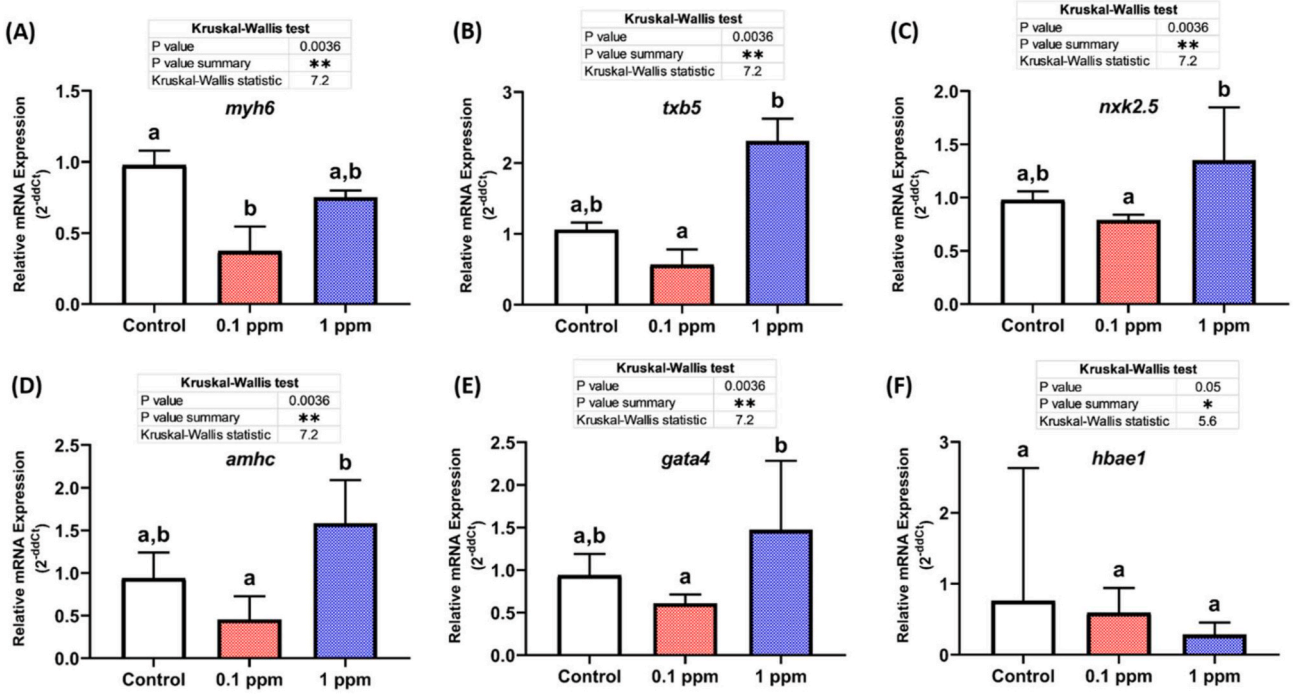

Fig. 10. The expression pattern of cardiovascular development-related genes (**(A)** *myh6*, **(B)** *txb5*, **(C)** *nxk2.5*, **(D)** *amhc*, **(E)** *gata4*, and **(F)** *hbae1*) in 3 dpf zebrafish larvae after exposed to CNTs for 1 day. The data were analyzed by using Kruskal-Wallis test, followed with Dunn's multiple comparisons test, and are presented as median with 95% CI. Different letters indicate a statistical difference ($P < 0.05$).

much more prominent D bands in MWCNTs. The RBM band (~200 cm^{-1}) is not present in MWCNTs because the outer tubes restrict the breathing mode. Considering the multilayer configuration, the more prominent D band in MWCNTs is to be expected to a certain extent and indicates more disorder in the structure [85]. As previously mentioned, the RBM mode completely disappears, and the I_D/I_G ratio is small. Therefore, the experimental results demonstrate that the test CNTs sample belongs to the MWCNTs. Next, the HRTEM results revealed that the test sample is MWCNTs since the diameter sizes of SWCNTs ranged from 0.8 to 5 nm [86]. In the case of CNTs, the nanotubes were typically observed with closed ends and somewhat smoother tube walls. Regarding the UV–vis results, the red shift suggests a bigger nanotube diameter for the used CNTs sample according to the reported correlation of the energy of the plasmon absorbance with mean SWNT diameter [73]. Further, the absorption bands at ~2920 and ~2854 cm^{-1} in FTIR signified the presence of alkyl chains in the CNTs [87]. The absorption band with a maximum at ~2360, ~1554, and ~1083 cm^{-1} are related to the *C*–O bond, the carboxylate anion stretch mode, and the stretching vibration of *C*–*O*–C, respectively [87–89]. The absorbance at ~1435 cm^{-1} is unique to MWCNTs, possibly due to the stretching vibration of aromatic C═C [87–89]. Finally, the zeta potential value found for pristine MWCNT is 0.75 mV [87]. Based on the FTIR results, the test MWCNTs sample may be treated with acids to introduce hydroxyl and carboxyl groups onto their surfaces [90]. Previously, CNTs' applications are frequently hampered by their limited dispersibility and solubility in different solvents. Thus, surface functionalization of CNTs has been utilized to overcome these limitations, however the extent of functionalization may also affect their toxicity [91]. Chemical functionalization with hydroxyl and carboxyl groups was demonstrated to increase the solubility and dispersion of CNTs, thus lowering their agglomeration tendency [92,93]. In a nanomaterials toxicity study, an aggregation of the particles in the solutions might reduce the effective dose of these materials, resulting in lower toxicity of the nanomaterials and misleading the researchers to be convinced that they are less hazardous than they may be [94]. Therefore, the toxicity of MWCNTs observed in the present study may be in the actual toxic level that this compound is expected to exert since particle aggregation was minimalized, although, the toxic effects might be different from pristine CNTs [95].

First, alterations were found in the tail coiling (TC) behaviors of the treated embryos. TC is the first locomotor activity of zebrafish embryos, developed in the pharyngula stage at 17 hpf as spontaneously one-sided tail coiling [96]. This movement is regulated by a single neural circuit located in the spinal cord and it has progressively been applied to evaluate the toxicities of various compounds [97–99]. Here, acute exposure to MWCNTs resulted in the reduction of zebrafish larval coiling activity, indicating that the MWCNTs could enter and reach the embryos since no agglomerates of MWCNTs adhered to the outer layer of the chorion of the embryos. This result is somewhat contrary to the previous finding that observed agglomerates of this compound in the outer layer of the zebrafish embryo's chorion. This difference might have occurred because the previous authors used MWCNTs with lengths greater than 2.5 μm while in the current study, MWCNTs with 19.7 nm of diameter were used [77]. In addition, another preliminary analysis also supports our hypothesis that the current MWCNTs crossed through the chorion since the pores of the chorion of 24 hpf zebrafish embryos were 0.23 μm [100,101]. The reduction in TC activity observed in our study might be due to the changes in neuromodulatory systems caused by MWCNTs. This assumption was based on the previous study that found SWCNTs affected cholinergic, serotonergic, and dopaminergic systems in the zebrafish brain, resulting in abnormal physiological and behavioral responses in the organism [102]. Disruption in the neuromodulatory system, especially the serotonergic system, had been suggested to be related to the absence of spontaneous tail movements at 24 hpf zebrafish as demonstrated by previous studies [48,103]. Furthermore, serotonin has been proven to play an important role as a signal molecule during crucial steps of early neurogenesis in zebrafish embryos, including the development of spinal motor neurons [104]. Additionally, the reduced frequency of spontaneous tail coiling might also be caused by the reduction of AChE enzyme activity, which is involved in the development of nerves, as mentioned in a prior study that demonstrated the high affinity of MWCNTs to AChE and AChE activity reductions caused by those nanotubes [105–107]. Taken together, our results indicated that MWCNTs may have a neurotoxic effect on the zebrafish embryos, as suggested by the significant hypoactivity reported.

Next, behavior alterations after exposure to MWCNTs were also observed during the larval stages of zebrafish in both locomotion assays. Similar to the tail coiling results, hypoactivity-like behavior was displayed by the low-concentration-treated group during the photomotor response assay. The PMR of zebrafish is a stereotypical series of motor behaviors in response to high-intensity light pulses and is regulated by multiple neurotransmitter pathways [108,109]. In general, zebrafish larval activity is higher during the light cycle than during the dark cycle, which was observed in all of the groups, even though the locomotion level of the treated groups was different from the control group [110]. This low activity of the low concentration-treated group is comparable to the prior study that found a depression of locomotor activity in 5 dpf zebrafish larvae during the spontaneous movement assay after being treated with both MWCNT-S (short, wide, and mostly dispersed) and MWCNT-L (long, thin, and agglomerated) in a range of concentrations. Interestingly, in their study, both MWCNTs were found to affect the larval locomotion in a dose-dependent manner, which was also similar to our results with a slightly higher locomotion activity of the high concentration-treated group than the untreated group during the dark cycle [77]. However, further experiments are required to study the dose-dependency effects of MWCNTs on zebrafish larval locomotion. Further, abnormalities were also observed during the VSRA. This assay was utilized to evaluate the startle and habituation of the larvae by observing their motor response after the repeated stimulation, which already demonstrated to meet the main criteria established for habituation [54]. Normally, zebrafish larvae display a high magnitude of a response to the first vibrational stimulus, allowing us to evaluate their escape response, followed by a decrease in the motor response after repeated exposure to the same vibrational stimuli that provide us the information on the habituation process of this response in those larvae [111]. Based on the results, even though both treated groups exhibited a similar escape response, MWCNTs statistically reduced habituation to vibrational startle response (VSR). This alteration might be elucidated by the MWCNTs' ability to bind to AChE, as mentioned above, since, a significant decrement in VSR habituation was also displayed by zebrafish larvae after being treated with an AChE inhibitor [54]. Furthermore, the altered locomotion observed in both tests may also be caused by the formation of reactive oxygen species (ROS) by MWCNTs. This speculation was based on the prior experiment of MWCNTs carried out on various animal models [23,112–114]. In those studies, MWCNTs enhanced the formation of ROS, which cause oxidative stress and oxidation and peroxidation of lipids, proteins, and DNA that can lead to significant cellular damage and even tissue or organ necrosis and failure [115]. As the brain contains high concentrations of polyunsaturated fatty acids that are highly susceptible to lipid peroxidation and lower activity of antioxidant enzymes that render the brain relatively deficient regarding antioxidant protection, the central nervous system is particularly vulnerable to oxidative stress [116,117]. Therefore, a high level of ROS might disrupt the brain development of fish and affect their swimming performance [118,119]. In conclusion, the changes in the larval movement after exposure to MWCNTs with the fact that the animals were alive indicate affection at the neuronal level or morphology anomalies that prevent the fish from swimming normally.

Oxygen consumption is a helpful physiological variable to measure the impacts of harmful substances on aquatic organisms. In terms of CNTs, their remarkable properties, such as their aspect ratios (length/width ratio) of >1000 and reactive surface chemistry, have caused concern about their biocompatibility, especially in the respiratory

system, which makes the assessment of general respiratory toxicity studies of this compound essential [120]. In the present study, disturbances in the respiratory system were observed in the larvae after being acutely treated with MWCNTs, manifested by increases in respiratory rate, especially in the high-concentration group. The increase in oxygen consumption is often associated with the increment in metabolism, as shown by the locomotion test results. In rodents, several experiments demonstrated the pulmonary toxicity of MWCNTs that was indicated by neutrophil inflammation or granulomatous formations in the lung, and persistent inflammation in the lung, which may be related to their various physical and chemical properties [75,120–123]. Meanwhile, in a SWCNTs study, the respiratory toxicity of these nanotubes was also observed in juvenile rainbow trout, characterized by signs of gill irritation, mucus secretion, and elevated ventilation rates. The gill injury observed at the end of the experiment indicated that the SWCNT had reached the sensitive gill epithelium and reduced respiratory efficiency. Taken together, the results suggested that MWCNTs caused respiratory stress in the zebrafish larvae by causing injuries in the larval gill. Thus, there is a need to conduct a histological examination of the larvae gills in future studies to verify this hypothesis.

Next, based on the cardiotoxicity results, the exposed larvae, especially in the low-concentration group, were found to exhibit similar results in terms of heart rhythm to the control group. This result is consistent with the prior study that found no obvious change in the heartbeats of larvae after being acutely exposed to MWCNTs in higher concentrations with significant reductions as the incubation time increased [22]. Another study also stated that these materials did not alter the cardiac rhythm of zebrafish in earlier life stages [124]. However, despite the current results on the heart rate of zebrafish larvae, obvious differences were shown during cardiac physiology and blood flow assessment, even though based on the pericardial cavity area measurement, no sign of edema was signified (Figs. S4F–I). To the best of our knowledge, this is the first report to show the MWCNTs' toxicities in zebrafish larval cardiac function. Nevertheless, a similar alteration was also demonstrated by a prior study in male SD rats with decrements in cardiac stroke work and stroke volume occurring with gradual dismissal at 1-day and 7-day post-exposure. Afterward, they proposed that pulmonary exposure to MWCNTs increased parasympathetic nervous activity as the mechanism of their cardiotoxicity [125]. Furthermore, this phenomenon might also be due to the alteration of NA^+/K^+-ATPase activity by MWCNTs. In zebrafish, the balance between ions, including potassium and calcium, is important to maintain a normal heart rhythm function as in humans [126]. While the transport and coordination of those ions are important for the stable action potential of cardiac myocytes, the maintenance of ion balance is regulated by ATP enzymes [127–129]. In fish, NA^+/K^+-ATPase is known for its role in ionic balance, and a previous study had shown that exposure to SWCNTs enhanced this protein in the gill of rainbow trout [130]. In addition, another research proved that MWCNTs interacting with cardiac myocytes can promote physiological growth and functional maturation in the neonatal rats by inducing some gene expressions, including sarcoplasmic reticulum Ca^{2+} ATPase 2a, which regulate the Ca^{2+} uptake and changes in its activity will affect cardiac function [131–134]. Taken together, the unbalanced of these enzymes might explain the cardiotoxicity observed in the present study.

Next, slower blood flow was also exhibited by exposed fish, especially in the low-dose group and this phenomenon could limit the supply of essential nutrients and gases that could alter the development of the larvae. The decreased blood flow speed was also observed in a prior experiment on zebrafish embryos after the microinjection of MWCNTs [100]. Furthermore, a group of researchers demonstrated platelet aggregation upon MWCNTs exposure [135]. Later, they suggested that the platelet activation was induced by regulating the intracellular Ca^{2+} concentration that plays a key role in the cellular signal transduction pathway, highlighting the thrombogenic properties of MWCNTs, which could form blot clots, disturbing the normal hemodynamics [136]. In addition, abnormal blood cells were also observed in most of the treated fishes, indicating the hemotoxicity of this compound (Video S1). This phenomenon is plausible considering the flow of nanoparticles that are highly affected by their uptake into blood macrophages and endothelial cells, which line the blood vessels through which nanoparticles flow along the body [137]. This finding is also supported by a previous study that found polystyrene nanoparticles (PS NPs) distribution throughout the bloodstream and accumulation in the heart region after being injected into the yolk sac of 2-days old zebrafish [138]. By using TEM, a previous finding showed that red blood cells with MWCNTs resulted in cell morphology distortions, loss of membrane smoothness, and shrinkage that in some cases led to membrane disruption in humans. Furthermore, the results indicated that the effects of MWCNTs on the larval blood flow are in a concentration-dependent manner. These toxic properties were quite similar to the toxicity of acid-functionalized SWCNTs (AF-SWCNTs). In a prior study, carboxylated SWCNTs were demonstrated to induce hemolysis on mouse red blood cells by binding to the erythrocyte membrane in a time- and concentration-dependent manner [136,139]. Since intravascular hemolysis is associated with blood flow regulation at the blood-contacting surface, the low blood flow speed observed in the present study may be due to the hemolysis caused by MWCNTs that require a deeper examination in the future [140,141]. Interestingly, after further investigation of the cardiovascular system of the treated larvae, abnormalities were found in their common cardinal vein (CCV), especially in the low-concentration group (Video S2). CCV, which grows across the yolk of zebrafish embryos, is extensively remodeled and regresses as the heart migrates dorsally within the pericardium [142]. However, an obvious delay in the CCV regression was observed in the low-concentration group. Since this is the first study to demonstrate this aberration, only a few supporting data could help elucidate this phenomenon. Despite that, similar findings had been demonstrated by some prior experiments in various nanoparticles and compounds, such as polyvinylpyrrolidone-coated silver nanoparticles (PVP-AgNPs), 2,3,7,8-tetrachlorodibenzo-p-dioxin (TCDD), 2, 2′,4,4′-Tetrabromodiphenyl ether (BDE-47) [142–144]. Based on those studies, we hypothesized that the MWCNTs changed the angiopoietin signaling that plays an essential role in modulating vascular remodeling and maturation during the development and delayed remodeling of CCV [145]. Nevertheless, more studies are needed to verify what mechanisms are involved in the cardio- and hemotoxicities of MWCNTs in zebrafish larvae.

Finally, yet importantly, despite all of the hypotheses regarding its cardiotoxicity mentioned above, several cardiovascular development-related genes were also investigated to help explain the mechanism underlying those phenomena. Here, the expression of *myh6*, a myocardia marker that promotes the expansion of ventricular myocardial cells, was slightly reduced in the low-concentration group [146]. Together with *myh7*, they are essential for heart muscle differentiation and specifically expressed in the atrium and the ventricle, respectively [147,148]. Alteration in the expression of this gene can cause toxicity to the heart in zebrafish larvae and eventually lead to death [149]. Interestingly, no irregular heart rhythm was observed in the present study, suggesting that the larvae were able to compensate for the slightly downregulated *myh6* at least 24 h post-administration. However, this abnormality may be related to the lower blood flow observed in the treated larvae. This hypothesis was taken based on a prior study in the chick embryo model that found atrial failure in *myh6*$^{-/-}$ mutant that resulted in reduced blood flow through the left ventricle and caused defects in the left ventricle morphogenesis [146,150]. This assumption was also supported by the relatively low expression level of *hbae1*, a hemoglobin marker gene, displayed by the treated larvae. The downregulation of this gene was also observed in the zebrafish embryos after knockdown of *C1q-like*, and morpholino knockdown of *C1qC* expression had been demonstrated to cause a premature return of caudal vein blood flow and failed to develop the more extended pattern of flow in the tail of embryos [151,152]. Nevertheless, based on those findings, these data

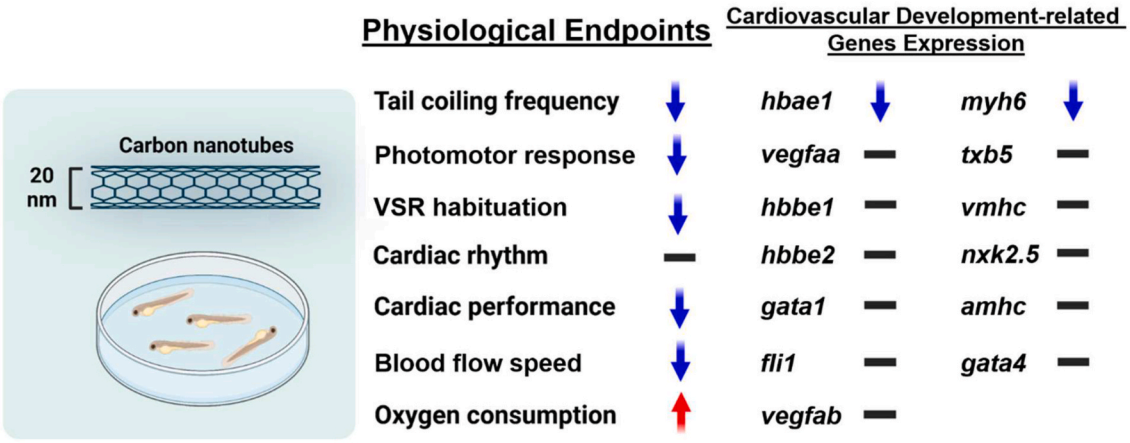

Fig. 11. Summary of the present study demonstrated various alterations that occurred in zebrafish larvae after carbon nanotubes (MWCNTs) exposure (↑: upregulated, ↓: downregulated, -: no significant change).

indicated that the tested MWCNTs might release their toxic effects on the embryonic hematopoietic process and impair the organization of mesencephalic vein and other brain blood vessels, which also could help in elucidating the behavior alterations displayed by the treated larvae in all of the tests. Lastly, the expression levels of several genes, which were t*xb5, nxk2.5, amhc,* and *gata4*, were lower in the low-concentration group compared to the high concentration group although both of them were not statistically different from the untreated group. In humans, these genes are critical for multiple events during heart development [153,154]. Furthermore, mutations of these genes have been demonstrated to induce a spectrum of heart malformations [155, 156]. Here, the results suggested that the tested MWCNTs, especially in the low concentration, caused disturbances in these important development transcription factors during a sensitive time window of development, resulting in more severe cardiac physiology alterations, which was indicated by a significantly low shortening fraction, than the high concentration group. In fetuses with cardiac defects, a low shortening fraction indicates cardiac decompensation, that indicate the heart inability to maintain and efficient circulation due to its abnormal condition, which might also explain the low velocity of blood flow observed in the low concentration treatment group [157,158]. Overall, the current results suggested that acute exposure to MWCNTs in the given concentrations statistically reduced the early expression of cardiac developmental genes, disturbing the homeostasis of cardiac physiology, and causing cardiac developmental toxicities.

5. Conclusions

To sum up, this finding clearly showed the environmental implications of acute exposure to MWCNTs in particularly low concentrations (Fig. 11). These MWCNTs released into the aquatic environment might pose hazards to the growth and survivability of aquatic animals through oral intake and long-term accumulation in organs. This issue will be a serious problem if MWCNTs harbor some environmental poisonous substances due to their large specific area and strong adsorption capability [159]. Furthermore, even though the larvae might successfully tolerate exposure for the first days, as shown in the present study, it is very unlikely that the risk of mortality would not be high after continuous exposure since it might disrupt their cardiovascular fitness or other routine behaviors performance in the wild [160]. However, future studies are needed to verify the risks and toxicity mechanism involved in chronic exposure to these nanoparticles to the health of aquatic animals.

Funding

This work was supported by the Ministry of Science and Technology [MOST 108-2313-B-033-001-MY3 and MOST 107-2622-B-033-001-CC2 to C.-D.H.

Author statement

Here, the toxicities of CNTs on aquatic animals, especially zebrafish, were assessed. The authors believed that this work is very important, considering the widely applied of this nanomaterial in various fields, which leads to the release of these CNTs into the aquatic environment. From the results, acute exposure to CNTs at relatively low concentrations resulted in neuro- and cardiotoxicities in zebrafish larvae, highlighting the hazards of this compound on aquatic organisms. The authors hoped that these findings provide a new perspective that improves our understanding of the hazards and risks of CNTs to the environment.

Declaration of competing interest

The authors declare that they have no known competing financial interests or personal relationships that could have appeared to influence the work reported in this paper.

Data availability

Data will be made available on request.

Acknowledgments

The authors thank Taiwan Zebrafish Core Facility at Academia Sinica (TZCAS) for providing the zebrafish AB strain. All authors reviewed the manuscript. The authors also appreciate the anonymous reviewers and editors for their professional comments, which improved the quality of this paper.

Appendix A. Supplementary data

Supplementary data to this article can be found online at https://doi.org/10.1016/j.cbi.2024.110925.

References

[1] I. Khan, K. Saeed, I. Khan, Nanoparticles: properties, applications and toxicities, Arab. J. Chem. 12 (2019) 908–931.
[2] K.S. Ibrahim, Carbon nanotubes-properties and applications: a review, Carbon Lett. 14 (2013) 131–144.

[3] Z. Peng, X. Liu, W. Zhang, Z. Zeng, Z. Liu, C. Zhang, Y. Liu, B. Shao, Q. Liang, W. Tang, Advances in the application, toxicity and degradation of carbon nanomaterials in environment: a review, Environ. Int. 134 (2020) 105298.

[4] W. Zhang, Z. Zhang, Y. Zhang, The application of carbon nanotubes in target drug delivery systems for cancer therapies, Nanoscale Res. Lett. 6 (2011) 1–22.

[5] G. Caruso, L. Merlo, E. Tot, C. Pignataro, M. Caffo, Nanotechnology and the New Frontiers of Drug Delivery in Cerebral Gliomas, Nano-And Microscale Drug Delivery Systems, Elsevier, 2017, pp. 95–112.

[6] S. Beg, M. Rahman, A. Jain, S. Saini, M. Hasnain, S. Swain, S. Imam, I. Kazmi, S. Akhter, Emergence in the Functionalized Carbon Nanotubes as Smart Nanocarriers for Drug Delivery Applications, Fullerens, Graphenes and Nanotubes, Elsevier, 2018, pp. 105–133.

[7] Y. Zhang, W. Bai, X. Cheng, J. Ren, W. Weng, P. Chen, X. Fang, Z. Zhang, H. Peng, Flexible and stretchable lithium-ion batteries and supercapacitors based on electrically conducting carbon nanotube fiber springs, Angew. Chem. Int. Ed. 53 (2014) 14564–14568.

[8] C. Hu, S. Hu, Carbon nanotube-based electrochemical sensors: principles and applications in biomedical systems, J. Sens. (2009) 2009.

[9] H. Yi, D. Huang, L. Qin, G. Zeng, C. Lai, M. Cheng, S. Ye, B. Song, X. Ren, X. Guo, Selective prepared carbon nanomaterials for advanced photocatalytic application in environmental pollutant treatment and hydrogen production, Appl. Catal. B Environ. 239 (2018) 408–424.

[10] J.M. Ngoy, N. Wagner, L. Riboldi, O. Bolland, A CO2 capture technology using multi-walled carbon nanotubes with polyaspartamide surfactant, Energy Proc. 63 (2014) 2230–2248.

[11] Q. Luo, H. Ma, Q. Hou, Y. Li, J. Ren, X. Dai, Z. Yao, Y. Zhou, L. Xiang, H. Du, Perovskite solar cells: all-carbon-electrode-based endurable flexible perovskite solar cells (adv. Funct. Mater. 11/2018, Adv. Funct. Mater. 28 (2018) 1870069.

[12] N.K. Mehra, A.K. Jain, M. Nahar, Carbon nanomaterials in oncology: an expanding horizon, Drug Discov. Today 23 (2018) 1016–1025.

[13] M. Mohajeri, B. Behnam, A. Sahebkar, Biomedical applications of carbon nanomaterials: drug and gene delivery potentials, J. Cell. Physiol. 234 (2019) 298–319.

[14] S. Mahajan, A. Patharkar, K. Kuche, R. Maheshwari, P.K. Deb, K. Kalia, R. K. Tekade, Functionalized carbon nanotubes as emerging delivery system for the treatment of cancer, Int. J. Pharm. 548 (2018) 540–558.

[15] D. Mohanta, S. Patnaik, S. Sood, N. Das, Carbon nanotubes: evaluation of toxicity at biointerfaces, J. Pharmaceu. Anal. 9 (2019) 293–300.

[16] K. Donaldson, R. Aitken, L. Tran, V. Stone, R. Duffin, G. Forrest, A. Alexander, Carbon nanotubes: a review of their properties in relation to pulmonary toxicology and workplace safety, Toxicol. Sci. 92 (2006) 5–22.

[17] C.-w. Lam, J.T. James, R. McCluskey, S. Arepalli, R.L. Hunter, A review of carbon nanotube toxicity and assessment of potential occupational and environmental health risks, Crit. Rev. Toxicol. 36 (2006) 189–217.

[18] A. Bianco, K. Kostarelos, C.D. Partidos, M. Prato, Biomedical applications of functionalised carbon nanotubes, Chem. Commun. (2005) 571–577.

[19] I. Schwyzer, R. Kaegi, L. Sigg, B. Nowack, Colloidal stability of suspended and agglomerate structures of settled carbon nanotubes in different aqueous matrices, Water Res. 47 (2013) 3910–3920.

[20] S. Lanone, P. Andujar, A. Kermanizadeh, J. Boczkowski, Determinants of carbon nanotube toxicity, Adv. Drug Deliv. Rev. 65 (2013) 2063–2069.

[21] A.A. Shvedova, A. Pietroiusti, B. Fadeel, V.E. Kagan, Mechanisms of carbon nanotube-induced toxicity: focus on oxidative stress, Toxicol. Appl. Pharmacol. 261 (2012) 121–133.

[22] X.T. Liu, X.Y. Mu, X.L. Wu, L.X. Meng, W.B. Guan, Y. Qiang, S. Hua, C.J. Wang, X. F. Li, Toxicity of multi-walled carbon nanotubes, graphene oxide, and reduced graphene oxide to zebrafish embryos, Biomed. Environ. Sci. 27 (2014) 676–683.

[23] K.R. Tavabe, M. Yavar, S. Kabir, P. Akbary, Z. Aminikhoei, Toxicity effects of multi-walled carbon nanotubes (MWCNTs) nanomaterial on the common carp (Cyprinus carpio L. 1758) in laboratory conditions, Comp. Biochem. Physiol. C Toxicol. Pharmacol. 237 (2020) 108832.

[24] J. Cheng, E. Flahaut, S.H. Cheng, Effect of carbon nanotubes on developing zebrafish (Danio rerio) embryos, Environ. Toxicol. Chem.: Int. J. 26 (2007) 708–716.

[25] J. Cheng, S.H. Cheng, Influence of carbon nanotube length on toxicity to zebrafish embryos, Int. J. Nanomed. 7 (2012) 3731.

[26] J. de Souza Filho, E.Y. Matsubara, L.P. Franchi, I.P. Martins, L.M.R. Rivera, J. M. Rosolen, C.K. Grisolia, Evaluation of carbon nanotubes network toxicity in zebrafish (Danio rerio) model, Environ. Res. 134 (2014) 9–16.

[27] J.W. Lee, Y.C. Choi, R. Kim, S.K. Lee, Multiwall carbon nanotube-induced apoptosis and antioxidant gene expression in the gills, liver, and intestine of Oryzias latipes, BioMed Res. Int. (2015) 2015 1-10.

[28] F. Gottschalk, T. Sonderer, R.W. Scholz, B. Nowack, Modeled environmental concentrations of engineered nanomaterials (TiO2, ZnO, Ag, CNT, fullerenes) for different regions, Environ. Sci. Technol. 43 (2009) 9216–9222.

[29] N.C. Mueller, B. Nowack, Exposure modeling of engineered nanoparticles in the environment, Environ. Sci. Technol. 42 (2008) 4447–4453.

[30] F. Schwab, T.D. Bucheli, L.P. Lukhele, A. Magrez, B. Nowack, L. Sigg, K. Knauer, Are carbon nanotube effects on green algae caused by shading and agglomeration? Environ. Sci. Technol. 45 (2011) 6136–6144.

[31] I.V. Mizgirev, S. Revskoy, A new zebrafish model for experimental leukemia therapy, Cancer Biol. Ther. 9 (2010) 895–902.

[32] D.-H. Pham, B. De Roo, X.-B. Nguyen, M. Vervaele, A. Kecskés, A. Ny, D. Copmans, H. Vriens, J.-P. Locquet, P. Hoet, Use of zebrafish larvae as a multi-endpoint platform to characterize the toxicity profile of silica nanoparticles, Sci. Rep. 6 (2016) 1–13.

[33] I. Munro, A. Renwick, B. Danielewska-Nikiel, The threshold of toxicological concern (TTC) in risk assessment, Toxicol. Lett. 180 (2008) 151–156.

[34] W. Liu, G. Huang, X. Su, S. Li, Q. Wang, Y. Zhao, Y. Liu, J. Luo, Y. Li, C. Li, Zebrafish: a promising model for evaluating the toxicity of carbon dot-based nanomaterials, ACS Appl. Mater. Interfaces 12 (2020) 49012–49020.

[35] H.-S. Han, G.H. Jang, I. Jun, H. Seo, J. Park, S. Glyn-Jones, H.-K. Seok, K.H. Lee, D. Mantovani, Y.-C. Kim, Transgenic zebrafish model for quantification and visualization of tissue toxicity caused by alloying elements in newly developed biodegradable metal, Sci. Rep. 8 (2018) 1–9.

[36] S. Cassar, I. Adatto, J.L. Freeman, J.T. Gamse, I. Iturria, C. Lawrence, A. Muriana, R.T. Peterson, S. Van Cruchten, L.I. Zon, Use of zebrafish in drug discovery toxicology, Chem. Res. Toxicol. 33 (2019) 95–118.

[37] A. Modarresi Chahardehi, H. Arsad, V. Lim, Zebrafish as a successful animal model for screening toxicity of medicinal plants, Plants 9 (2020) 1345.

[38] A.J. Hill, H. Teraoka, W. Heideman, R.E. Peterson, Zebrafish as a model vertebrate for investigating chemical toxicity, Toxicol. Sci. 86 (2005) 6–19.

[39] A. Avdesh, M. Chen, M.T. Martin-Iverson, A. Mondal, D. Ong, S. Rainey-Smith, K. Taddei, M. Lardelli, D.M. Groth, G. Verdile, Regular care and maintenance of a zebrafish (Danio rerio) laboratory: an introduction, JoVE (2012) e4196.

[40] H. Wu, G. Liu, Y. Zhuang, D. Wu, H. Zhang, H. Yang, H. Hu, S. Yang, The behavior after intravenous injection in mice of multiwalled carbon nanotube/Fe3O4 hybrid MRI contrast agents, Biomaterials 32 (2011) 4867–4876.

[41] S. Ivani, I. Karimi, S.R.F. Tabatabaei, Biosafety of multiwalled carbon nanotube in mice: a behavioral toxicological approach, J. Toxicol. Sci. 37 (2012) 1191–1205.

[42] J. Muller, M. Delos, N. Panin, V. Rabolli, F. Huaux, D. Lison, Absence of carcinogenic response to multiwall carbon nanotubes in a 2-year bioassay in the peritoneal cavity of the rat, Toxicol. Sci. 110 (2009) 442–448.

[43] H.M. Maes, F. Stibany, S. Giefers, B. Daniels, B.r. Deutschmann, W. Baumgartner, A. Schäffer, Accumulation and distribution of multiwalled carbon nanotubes in zebrafish (Danio rerio), Environ. Sci. Technol. 48 (2014) 12256–12264.

[44] A.A. Adenuga, L. Truong, R.L. Tanguay, V.T. Remcho, Preparation of water soluble carbon nanotubes and assessment of their biological activity in embryonic zebrafish, Int. J. Biomed. Nanosci. Nanotechnol. (IJBNN) 3 (2013) 38–51.

[45] L.M. Gilbertson, F. Melnikov, L.C. Wehmas, P.T. Anastas, R.L. Tanguay, J. B. Zimmerman, Toward safer multi-walled carbon nanotube design: establishing a statistical model that relates surface charge and embryonic zebrafish mortality, Nanotoxicology 10 (2016) 10–19.

[46] S.B. Lovern, R. Klaper, Daphnia magna mortality when exposed to titanium dioxide and fullerene (C60) nanoparticles, Environ. Toxicol. Chem.: Int. J. 25 (2006) 1132–1137.

[47] K.A. Kurnia, F. Santoso, B.P. Sampurna, G. Audira, J.-C. Huang, K.H.-C. Chen, C.-D. Hsiao, TCMacro: a simple and robust ImageJ-based method for automated measurement of tail coiling activity in zebrafish, Biomolecules 11 (2021) 1133.

[48] F. Zindler, F. Beedgen, D. Brandt, M. Steiner, D. Stengel, L. Baumann, T. Braunbeck, Analysis of tail coiling activity of zebrafish (Danio rerio) embryos allows for the differentiation of neurotoxicants with different modes of action, Ecotoxicol. Environ. Saf. 186 (2019) 109754.

[49] A.O. Ogungbemi, E. Teixido, R. Massei, S. Scholz, E. Küster, Optimization of the spontaneous tail coiling test for fast assessment of neurotoxic effects in the zebrafish embryo using an automated workflow in KNIME®, Neurotoxicol. Teratol. 81 (2020) 106918.

[50] L. Sullivan, Power and Sample Size Determination, Boston Univeristy School of Public Health, Boston, MA, USA, 2017.

[51] L.A. Kristofco, L.C. Cruz, S.P. Haddad, M.L. Behra, C.K. Chambliss, B.W. Brooks, Age matters: developmental stage of Danio rerio larvae influences photomotor response thresholds to diazinion or diphenhydramine, Aquat. Toxicol. 170 (2016) 344–354.

[52] P. Siregar, G. Audira, L.-Y. Feng, J.-H. Lee, F. Santoso, W.-H. Yu, Y.-H. Lai, J.-H. Li, Y.-T. Lin, J.-R. Chen, Pharmaceutical assessment suggests locomotion hyperactivity in zebrafish triggered by arecoline might Be associated with multiple muscarinic acetylcholine receptors activation, Toxins 13 (2021) 259.

[53] Y. Liu, R. Carmer, G. Zhang, P. Venkatraman, S.A. Brown, C.-P. Pang, M. Zhang, P. Ma, Y.F. Leung, Statistical analysis of zebrafish locomotor response, PLoS One 10 (2015) e0139521.

[54] M. Faria, E. Prats, K.A. Novoa-Luna, J. Bedrossiantz, C. Gómez-Canela, L. M. Gómez-Oliván, D. Raldúa, Development of a vibrational startle response assay for screening environmental pollutants and drugs impairing predator avoidance, Sci. Total Environ. 650 (2019) 87–96.

[55] M. Faria, J. Bedrossiantz, E. Prats, X.R. Garcia, C. Gómez-Canela, B. Piña, D. Raldúa, Deciphering the mode of action of pollutants impairing the fish larvae escape response with the vibrational startle response assay, Sci. Total Environ. 672 (2019) 121–128.

[56] B. Bagatto, B. Pelster, W. Burggren, Growth and metabolism of larval zebrafish: effects of swim training, J. Exp. Biol. 204 (2001) 4335–4343.

[57] G. Del Vecchio, K. Murashita, T. Verri, A.S. Gomes, I. Rønnestad, Leptin receptor-deficient (knockout) zebrafish: effects on nutrient acquisition, Gen. Comp. Endocrinol. 310 (2021) 113832.

[58] P. Rombough, H. Drader, Hemoglobin enhances oxygen uptake in larval zebrafish (Danio rerio) but only under conditions of extreme hypoxia, J. Exp. Biol. 212 (2009) 778–784.

[59] F. Saputra, Y.-H. Lai, R.A.T. Fernandez, A.P.G. Macabeo, H.-T. Lai, J.-C. Huang, C.-D. Hsiao, Acute and sub-chronic exposure to artificial sweeteners at the highest environmentally relevant concentration induce less cardiovascular physiology alterations in zebrafish larvae, Biology 10 (2021) 548.

[60] B.P. Sampurna, G. Audira, S. Juniardi, Y.-H. Lai, C.-D. Hsiao, A simple ImageJ-based method to measure cardiac rhythm in zebrafish embryos, Inventions 3 (2018) 21.
[61] F. Saputra, B. Uapipatanakul, J.-S. Lee, S.-M. Hung, J.-C. Huang, Y.-C. Pang, J.E. R. Muñoz, A.P.G. Macabeo, K.H.-C. Chen, C.-D. Hsiao, Co-treatment of copper oxide nanoparticle and carbofuran enhances cardiotoxicity in zebrafish embryos, Int. J. Mol. Sci. 22 (2021) 8259.
[62] F. Santoso, B.P. Sampurna, Y.-H. Lai, S.-T. Liang, E. Hao, J.-R. Chen, C.-D. Hsiao, Development of a simple imagej-based method for dynamic blood flow tracking in zebrafish embryos and its application in drug toxicity evaluation, Inventions 4 (2019) 65.
[63] Y. Han, J.p. Zhang, J.q. Qian, C.q. Hu, Cardiotoxicity evaluation of anthracyclines in zebrafish (Danio rerio), J. Appl. Toxicol. 35 (2015) 241–252.
[64] E. Perumal, S. Eswaran, R. Parvin, S. Balasubramanian, Mitigation of arsenic induced developmental cardiotoxicity by ferulic acid in zebrafish, Comparative Biochemistry and Physiology Part C, Toxicol. & Pharmacol. 244 (2021) 109021.
[65] K.J. Livak, T.D. Schmittgen, Analysis of relative gene expression data using real-time quantitative PCR and the 2− ΔΔCT method, Methods 25 (2001) 402–408.
[66] H. Liu, T. Chu, L. Chen, W. Gui, G. Zhu, In vivo cardiovascular toxicity induced by acetochlor in zebrafish larvae, Chemosphere 181 (2017) 600–608.
[67] D.C. Adams, C.D. Anthony, Using randomization techniques to analyse behavioural data, Anim. Behav. 51 (1996) 733–738.
[68] J. Oddershede, K. Nielsen, K. Stahl, Using X-ray powder diffraction and principal component analysis to determine structural properties for bulk samples of multiwall carbon nanotubes, Z. für Kristallogr. - Cryst. Mater. 222 (2007) 186–192.
[69] P. Lambin, A. Loiseau, C. Culot, L. Biro, Structure of carbon nanotubes probed by local and global probes, Carbon 40 (2002) 1635–1648.
[70] R. Das, S. Bee Abd Hamid, M. Eaqub Ali, S. Ramakrishna, W. Yongzhi, Carbon nanotubes characterization by X-ray powder diffraction–a review, Curr. Nanosci. 11 (2015) 23–35.
[71] N.O. Ramoraswi, P.G. Ndungu, Photo-catalytic properties of TiO 2 supported on MWCNTs, SBA-15 and silica-coated MWCNTs nanocomposites, Nanoscale Res. Lett. 10 (2015) 1–16.
[72] T.G. Pedersen, Variational approach to excitons in carbon nanotubes, Phys. Rev. B 67 (2003) 073401.
[73] G.A. Rance, D.H. Marsh, R.J. Nicholas, A.N. Khlobystov, UV–vis absorption spectroscopy of carbon nanotubes: relationship between the π-electron plasmon and nanotube diameter, Chem. Phys. Lett. 493 (2010) 19–23.
[74] C.-W. Lam, J.T. James, R. McCluskey, R.L. Hunter, Pulmonary toxicity of single-wall carbon nanotubes in mice 7 and 90 days after intratracheal instillation, Toxicol. Sci. 77 (2004) 126–134.
[75] J. Muller, F. Huaux, N. Moreau, P. Misson, J.-F. Heilier, M. Delos, M. Arras, A. Fonseca, J.B. Nagy, D. Lison, Respiratory toxicity of multi-wall carbon nanotubes, Toxicol. Appl. Pharmacol. 207 (2005) 221–231.
[76] D.B. Warheit, B.R. Laurence, K.L. Reed, D.H. Roach, G.A. Reynolds, T.R. Webb, Comparative pulmonary toxicity assessment of single-wall carbon nanotubes in rats, Toxicol. Sci. 77 (2004) 117–125.
[77] C. Martinez, D. Igartúa, I. Czarnowski, D. Feas, M. Prieto, Biological response and developmental toxicity of zebrafish embryo and larvae exposed to multi-walled carbon nanotubes with different dimension, Heliyon 5 (2019) e02308.
[78] M. Allegri, D.K. Perivoliotis, M.G. Bianchi, M. Chiu, A. Pagliaro, M.A. Koklioti, A.-F.A. Trompeta, E. Bergamaschi, O. Bussolati, C.A. Charitidis, Toxicity determinants of multi-walled carbon nanotubes: the relationship between functionalization and agglomeration, Toxicol Rep 3 (2016) 230–243.
[79] F.I. Aksakal, A. Ciltas, N.S. Ozek, A holistic study on potential toxic effects of carboxylated multi-walled carbon nanotubes (MWCNTs-COOH) on zebrafish (Danio rerio) embryos/larvae, Chemosphere 225 (2019) 820–828.
[80] A. Sayah, F. Habelhames, A. Bahloul, B. Nessark, Y. Bonnassieux, D. Tendelier, M. El Jouad, Electrochemical synthesis of polyaniline-exfoliated graphene composite films and their capacitance properties, J. Electroanal. Chem. 818 (2018) 26–34.
[81] T. Belin, F. Epron, Characterization methods of carbon nanotubes: a review, Mater. Sci. Eng., B 119 (2005) 105–118.
[82] R. Paul, A.K. Mitra, Photoluminescence from SWCNT/Cu Hybrid Nanostructure Synthesized by a Soft Chemical Route, International Scholarly Research Notices, 2012, 2012.
[83] A.J. Haider, M. Mohammed, D.S. Ahmed, Preparation and characterization of multi walled carbon naotubes/Ag nanoparticles hybrid materials, Int. J. Sci. Eng. Res. 5 (2014).
[84] Y.C. Choi, K.-I. Min, M.S. Jeong, Novel method of evaluating the purity of multiwall carbon nanotubes using Raman spectroscopy, J. Nanomater. (2013) 2013.
[85] Y. Piao, V.N. Tondare, C.S. Davis, J.M. Gorham, E.J. Petersen, J.W. Gilman, K. Scott, A.E. Vladár, A.R.H. Walker, Comparative study of multiwall carbon nanotube nanocomposites by Raman, SEM, and XPS measurement techniques, Compos. Sci. Technol. 208 (2021) 108753.
[86] A. Al-zubaidi, N. Asai, Y. Ishii, S. Kawasaki, The effect of diameter size of single-walled carbon nanotubes on their high-temperature energy storage behaviour in ionic liquid-based electric double-layer capacitors, RSC Adv. 10 (2020) 41209–41216.
[87] T.L. do Amaral Montanheiro, F.H. Cristóvan, J.P.B. Machado, D.B. Tada, N. Durán, A.P. Lemes, Effect of MWCNT functionalization on thermal and electrical properties of PHBV/MWCNT nanocomposites, J. Mater. Res. 30 (2015) 55–65.
[88] A. Misra, P.K. Tyagi, P. Rai, D. Misra, FTIR spectroscopy of multiwalled carbon nanotubes: a simple approachto study the nitrogen doping, J. Nanosci. Nanotechnol. 7 (2007) 1820–1823.
[89] R.N. Oliveira, M.C. Mancini, F.C.S.d. Oliveira, T.M. Passos, B. Quilty, R.M.d.S. M. Thiré, G.B. McGuinness, FTIR analysis and quantification of phenols and flavonoids of five commercially available plants extracts used in wound healing, Materia 21 (2016) 767–779.
[90] J.M. Huang, M.F. Tsai, S.J. Yang, W.M. Chiu, Preparation and thermal properties of multiwalled carbon nanotube/polybenzoxazine nanocomposites, J. Appl. Polym. Sci. 122 (2011) 1898–1904.
[91] J.H. Lehman, M. Terrones, E. Mansfield, K.E. Hurst, V. Meunier, Evaluating the characteristics of multiwall carbon nanotubes, Carbon 49 (2011) 2581–2602.
[92] T. Coccini, E. Roda, D. Sarigiannis, P. Mustarelli, E. Quartarone, A. Profumo, L. Manzo, Effects of water-soluble functionalized multi-walled carbon nanotubes examined by different cytotoxicity methods in human astrocyte D384 and lung A549 cells, Toxicology 269 (2010) 41–53.
[93] M. Bottini, S. Bruckner, K. Nika, N. Bottini, S. Bellucci, A. Magrini, A. Bergamaschi, T. Mustelin, Multi-walled carbon nanotubes induce T lymphocyte apoptosis, Toxicol. Lett. 160 (2006) 121–126.
[94] M.M. Falinski, M.A. Garland, S.M. Hashmi, R.L. Tanguay, J.B. Zimmerman, Establishing structure-property-hazard relationships for multi-walled carbon nanotubes: the role of aggregation, surface charge, and oxidative stress on embryonic zebrafish mortality, Carbon 155 (2019) 587–600.
[95] C.L. Ursini, D. Cavallo, A.M. Fresegna, A. Ciervo, R. Maiello, S. Casciardi, F. Tombolini, G. Buresti, S. Iavicoli, Study of cytotoxic and genotoxic effects of hydroxyl-functionalized multiwalled carbon nanotubes on human pulmonary cells, J. Nanomater. (2012) 2012.
[96] L. Saint-Amant, P. Drapeau, Time course of the development of motor behaviors in the zebrafish embryo, J. Neurobiol. 37 (1998) 622–632.
[97] L. Saint-Amant, P. Drapeau, Motoneuron activity patterns related to the earliest behavior of the zebrafish embryo, J. Neurosci. 20 (2000) 3964–3972.
[98] S.M. Vliet, T.C. Ho, D.C. Volz, Behavioral screening of the LOPAC1280 library in zebrafish embryos, Toxicol. Appl. Pharmacol. 329 (2017) 241–248.
[99] H. Richendrfer, R. Creton, R.M. Colwill, The Embryonic Zebrafish as a Model System to Study the Effects of Environmental Toxicants on Behavior, Zebrafish, Nova Science Publishers, New York, NY, USA, 2014, pp. 245–264.
[100] P. Asharani, N. Serina, M. Nurmawati, Y.L. Wu, Z. Gong, S. Valiyaveettil, Impact of multi-walled carbon nanotubes on aquatic species, J. Nanosci. Nanotechnol. 8 (2008) 3603–3609.
[101] K.E. Pelka, K. Henn, A. Keck, B. Sapel, T. Braunbeck, Size does matter–Determination of the critical molecular size for the uptake of chemicals across the chorion of zebrafish (Danio rerio) embryos, Aquat. Toxicol. 185 (2017) 1–10.
[102] A. Da Rocha, L. Kist, E. Almeida, D. Silva, C. Bonan, S. Altenhofen, C. Kaufmann Jr., M. Bogo, D. Barros, S. Oliveira, Neurotoxicity in zebrafish exposed to carbon nanotubes: effects on neurotransmitters levels and antioxidant system, Comp. Biochem. Physiol. C Toxicol. Pharmacol. 218 (2019) 30–35.
[103] M.D. McDonald, An AOP analysis of selective serotonin reuptake inhibitors (SSRIs) for fish, Comp. Biochem. Physiol. C Toxicol. Pharmacol. 197 (2017) 19–31.
[104] A. Barreiro-Iglesias, K.S. Mysiak, A.L. Scott, M.M. Reimer, Y. Yang, C.G. Becker, T. Becker, Serotonin promotes development and regeneration of spinal motor neurons in zebrafish, Cell Rep. 13 (2015) 924–932.
[105] Z. Wang, J. Zhao, F. Li, D. Gao, B. Xing, Adsorption and inhibition of acetylcholinesterase by different nanoparticles, Chemosphere 77 (2009) 67–73.
[106] L. De Marchi, V. Neto, C. Pretti, E. Figueira, F. Chiellini, A. Morelli, A.M. Soares, R. Freitas, Effects of multi-walled carbon nanotube materials on Ruditapes philippinarum under climate change: the case of salinity shifts, Aquat. Toxicol. 199 (2018) 199–211.
[107] H. Wang, L. Zhou, X. Liao, Z. Meng, J. Xiao, F. Li, S. Zhang, Z. Cao, H. Lu, Toxic effects of oxine-copper on development and behavior in the embryo-larval stages of zebrafish, Aquat. Toxicol. 210 (2019) 242–250.
[108] D. Kokel, J. Bryan, C. Laggner, R. White, C.Y.J. Cheung, R. Mateus, D. Healey, S. Kim, A.A. Werdich, S.J. Haggarty, Rapid behavior-based identification of neuroactive small molecules in the zebrafish, Nat. Chem. Biol. 6 (2010) 231–237.
[109] D. Copmans, T. Meinl, C. Dietz, M. van Leeuwen, J. Ortmann, M.R. Berthold, P. A. de Witte, A KNIME-based analysis of the zebrafish photomotor response clusters the phenotypes of 14 classes of neuroactive molecules, J. Biomol. Screen 21 (2016) 427–436.
[110] R.C. MacPhail, D.L. Hunter, T.D. Irons, S. Padilla, Locomotion and behavioral toxicity in larval zebrafish: background, methods, and data, Zebrafish: Methods for Assessing Drug Safety and Toxicity (2011) 151–164.
[111] M. Faria, X. Wu, M. Luja-Mondragón, E. Prats, L.M. Gómez-Oliván, B. Piña, D. Raldúa, Screening anti-predator behaviour in fish larvae exposed to environmental pollutants, Sci. Total Environ. 714 (2020) 136759.
[112] R. Saria, F. Mouchet, A. Perrault, E. Flahaut, C. Laplanche, J.-C. Boutonnet, E. Pinelli, L. Gauthier, Short term exposure to multi-walled carbon nanotubes induce oxidative stress and DNA damage in Xenopus laevis tadpoles, Ecotoxicol. Environ. Saf. 107 (2014) 22–29.
[113] S. Amjad, A. Sharma, M. Serajuddin, Toxicity assessment of cypermethrin nanoparticles in Channa punctatus: behavioural response, micronuclei induction and enzyme alteration, Regul. Toxicol. Pharmacol. 100 (2018) 127–133.
[114] J.P. Souza, A.S. Mansano, F.P. Venturini, F. Santos, V. Zucolotto, Antioxidant metabolism of zebrafish after sub-lethal exposure to graphene oxide and recovery, Fish Physiol. Biochem. 45 (2019) 1289–1297.

[115] A. Tripathy, Oxidative stress, reactive oxygen species (ROS) and antioxidative defense system, with special reference to fish, Int. J. Curr. Res. Biosci. Plant Biol. 3 (2016) 79–89.
[116] E. Mariani, M. Polidori, A. Cherubini, P. Mecocci, Oxidative stress in brain aging, neurodegenerative and vascular diseases: an overview, J. Chromatogr. B 827 (2005) 65–75.
[117] B. Zhu, Q. Wang, X. Shi, Y. Guo, T. Xu, B. Zhou, Effect of combined exposure to lead and decabromodiphenyl ether on neurodevelopment of zebrafish larvae, Chemosphere 144 (2016) 1646–1654.
[118] L.E. Salminen, R.H. Paul, Oxidative stress and genetic markers of suboptimal antioxidant defense in the aging brain: a theoretical review, Rev. Neurosci. 25 (2014) 805–819.
[119] Q. Chen, M. Gundlach, S. Yang, J. Jiang, M. Velki, D. Yin, H. Hollert, Quantitative investigation of the mechanisms of microplastics and nanoplastics toward zebrafish larvae locomotor activity, Sci. Total Environ. 584 (2017) 1022–1031.
[120] L. Ma-Hock, S. Treumann, V. Strauss, S. Brill, F. Luizi, M. Mertler, K. Wiench, A. O. Gamer, B. Van Ravenzwaay, R. Landsiedel, Inhalation toxicity of multiwall carbon nanotubes in rats exposed for 3 months, Toxicol. Sci. 112 (2009) 468–481.
[121] Y. Morimoto, M. Hirohashi, A. Ogami, T. Oyabu, T. Myojo, M. Todoroki, M. Yamamoto, M. Hashiba, Y. Mizuguchi, B.W. Lee, Pulmonary toxicity of well-dispersed multi-wall carbon nanotubes following inhalation and intratracheal instillation, Nanotoxicology 6 (2012) 587–599.
[122] N. Kobayashi, M. Naya, M. Ema, S. Endoh, J. Maru, K. Mizuno, J. Nakanishi, Biological response and morphological assessment of individually dispersed multi-wall carbon nanotubes in the lung after intratracheal instillation in rats, Toxicology 276 (2010) 143–153.
[123] Y. Morimoto, M. Horie, N. Kobayashi, N. Shinohara, M. Shimada, Inhalation toxicity assessment of carbon-based nanoparticles, Accounts Chem. Res. 46 (2013) 770–781.
[124] S. Wang, C. Zhuang, J. Du, C. Wu, H. You, The presence of MWCNTs reduces developmental toxicity of PFOS in early life stage of zebrafish, Environ. Pollut. 222 (2017) 201–209.
[125] W. Zheng, W. McKinney, M.L. Kashon, D. Pan, V. Castranova, H. Kan, The effects of inhaled multi-walled carbon nanotubes on blood pressure and cardiac function, Nanoscale Res. Lett. 13 (2018) 1–9.
[126] A. Pott, W. Rottbauer, S. Just, Functional genomics in zebrafish as a tool to identify novel antiarrhythmic targets, Curr. Med. Chem. 21 (2014) 1320–1329.
[127] Y. Xu, Z. Zhang, V. Timofeyev, D. Sharma, D. Xu, D. Tuteja, P.H. Dong, G. U. Ahmmed, Y. Ji, G.E. Shull, The effects of intracellular Ca2+ on cardiac K+ channel expression and activity: novel insights from genetically altered mice, J. Physiol. 562 (2005) 745–758.
[128] V. Yadwad, V. Kallapur, S. Basalingappa, Inhibition of gill Na+ K+-ATPase activity in dragonfly larva, Pantala flavescens, by endosulfan, Bull. Environ. Contam. Toxicol. 44 (1990) 585–589.
[129] J.G. Richards, J.W. Semple, J.S. Bystriansky, P.M. Schulte, Na+/K+-ATPase α-isoform switching in gills of rainbow trout (Oncorhynchus mykiss) during salinity transfer, J. Exp. Biol. 206 (2003) 4475–4486.
[130] C.J. Smith, B.J. Shaw, R.D. Handy, Toxicity of single walled carbon nanotubes to rainbow trout,(Oncorhynchus mykiss): respiratory toxicity, organ pathologies, and other physiological effects, Aquat. Toxicol. 82 (2007) 94–109.
[131] L. Mestroni, V. Martinelli, G. Cellot, F.M. Toma, C. Long, J. Caldwell, L. Zentilin, M. Giacca, A. Turco, M. Prato, Carbon nanotubes instruct physiological growth and functionally mature syncytia: non-genetic engineering of cardiac myocytes, J. Am. Coll. Cardiol. 61 (2013). E567-E567.
[132] Y. Xu, X. Li, M. Zhou, Neuregulin-1/ErbB signaling: a druggable target for treating heart failure, Curr. Opin. Pharmacol. 9 (2009) 214–219.
[133] I.F. Kodde, J. van der Stok, R.T. Smolenski, J.W. de Jong, Metabolic and genetic regulation of cardiac energy substrate preference, Comp. Biochem. Physiol. Mol. Integr. Physiol. 146 (2007) 26–39.
[134] Y. Wu, Y. Zhang, M. Chen, Q. Yang, S. Zhuang, L. Lv, Z. Zuo, C. Wang, Exposure to low-level metalaxyl impacts the cardiac development and function of zebrafish embryos, J. Environ. Sci. 85 (2019) 1–8.
[135] G.F. Guidetti, A. Consonni, L. Cipolla, P. Mustarelli, C. Balduini, M. Torti, Nanoparticles induce platelet activation in vitro through stimulation of canonical signalling pathways, Nanomed. Nanotechnol. Biol. Med. 8 (2012) 1329–1336.
[136] C. Bussy, L. Methven, K. Kostarelos, Hemotoxicity of carbon nanotubes, Adv. Drug Deliv. Rev. 65 (2013) 2127–2134.
[137] N.J.K. Dal, A. Kocere, J. Wohlmann, S. Van Herck, T.A. Bauer, J. Resseguier, S. Bagherifam, H. Hyldmo, M. Barz, B.G. De Geest, Zebrafish embryos allow prediction of nanoparticle circulation times in mice and facilitate quantification of nanoparticle–cell interactions, Small 16 (2020) 1906719.
[138] J.A. Pitt, J.S. Kozal, N. Jayasundara, A. Massarsky, R. Trevisan, N. Geitner, M. Wiesner, E.D. Levin, R.T. Di Giulio, Uptake, tissue distribution, and toxicity of polystyrene nanoparticles in developing zebrafish (Danio rerio), Aquat. Toxicol. 194 (2018) 185–194.
[139] S. Sachar, R.K. Saxena, Cytotoxic effect of poly-dispersed single walled carbon nanotubes on erythrocytes in vitro and in vivo, PLoS One 6 (2011) e22032.
[140] T. Yasuda, K. Shimokasa, A. Funakubo, T. Higami, T. Kawamura, Y. Fukui, An investigation of blood flow behavior and hemolysis in artificial organs, Am. Soc. Artif. Intern. Organs J. 46 (2000) 527–531.
[141] R. Grygorczyk, S.N. Orlov, Effects of hypoxia on erythrocyte membrane properties—implications for intravascular hemolysis and purinergic control of blood flow, Front. Physiol. 8 (2017) 1110.
[142] J. Gao, C.T. Mahapatra, C.D. Mapes, M. Khlebnikova, A. Wei, M.S. Sepúlveda, Vascular toxicity of silver nanoparticles to developing zebrafish (Danio rerio), Nanotoxicology 10 (2016) 1363–1372.
[143] S. Bello, W. Heideman, R. Peterson, 2, 3, 7, 8-Tetrachlorodibenzo-p-dioxin inhibits regression of the common cardinal vein in developing zebrafish, Toxicol. Sci. 78 (2004) 258–266.
[144] X. Xing, J. Kang, J. Qiu, X. Zhong, X. Shi, B. Zhou, Y. Wei, Waterborne exposure to low concentrations of BDE-47 impedes early vascular development in zebrafish embryos/larvae, Aquat. Toxicol. 203 (2018) 19–27.
[145] V.N. Pham, B.L. Roman, B.M. Weinstein, Isolation and expression analysis of three zebrafish angiopoietin genes, Dev. Dynam.: Off. Publ. Am. Assoc. Anatomists 221 (2001) 470–474.
[146] P. Sarantis, C. Gaitanaki, D. Beis, Ventricular remodeling of single-chambered myh6−/− adult zebrafish hearts occurs via a hyperplastic response and is accompanied by elastin deposition in the atrium, Cell Tissue Res. 378 (2019) 279–288.
[147] D. Yelon, S.A. Horne, D.Y. Stainier, Restricted expression of cardiac myosin genes reveals regulated aspects of heart tube assembly in zebrafish, Dev. Biol. 214 (1999) 23–37.
[148] E. Berdougo, H. Coleman, D.H. Lee, D.Y. Stainier, D. Yelon, Mutation of Weak Atrium/atrial Myosin Heavy Chain Disrupts Atrial Function and Influences Ventricular Morphogenesis in Zebrafish, 2003.
[149] M. Li, L. Yao, H. Chen, X. Ni, Y. Xu, W. Dong, M. Fang, D. Chen, L. Xu, B. Zhao, Chiral toxicity of muscone to embryonic zebrafish heart, Aquat. Toxicol. 222 (2020) 105451.
[150] D. Sedmera, N. Hu, K.M. Weiss, B.B. Keller, S. Denslow, R.P. Thompson, Cellular changes in experimental left heart hypoplasia, Anat. Rec.: Off. Publ. Am. Assoc. Anatomists 267 (2002) 137–145.
[151] J. Mei, Q.-Y. Zhang, Z. Li, S. Lin, J.-F. Gui, C1q-like inhibits p53-mediated apoptosis and controls normal hematopoiesis during zebrafish embryogenesis, Dev. Biol. 319 (2008) 273–284.
[152] M.A. Pickart, E.W. Klee, A.L. Nielsen, S. Sivasubbu, E.M. Mendenhall, B.R. Bill, E. Chen, C.E. Eckfeldt, M. Knowlton, M.E. Robu, Genome-wide reverse genetics framework to identify novel functions of the vertebrate secretome, PLoS One 1 (2006) e104.
[153] P. Zhou, A. He, W.T. Pu, Regulation of GATA4 transcriptional activity in cardiovascular development and disease, Curr. Top. Dev. Biol. 100 (2012) 143–169.
[154] F. Greulich, C. Rudat, A. Kispert, Mechanisms of T-box gene function in the developing heart, Cardiovasc. Res. 91 (2011) 212–222.
[155] C.T. Basson, D.R. Bachinsky, R.C. Lin, T. Levi, J.A. Elkins, J. Soults, D. Grayzel, E. Kroumpouzou, T.A. Traill, J. Leblanc-Straceski, Mutations in human cause limb and cardiac malformation in Holt-Oram syndrome, Nat. Genet. 15 (1997) 30–35.
[156] V. Garg, I.S. Kathiriya, R. Barnes, M.K. Schluterman, I.N. King, C.A. Butler, C. R. Rothrock, R.S. Eapen, K. Hirayama-Yamada, K. Joo, GATA4 mutations cause human congenital heart defects and reveal an interaction with TBX5, Nature 424 (2003) 443–447.
[157] T. Tongsong, C. Wanapirak, W. Piyamongkol, S. Sirichotiyakul, F. Tongprasert, K. Srisupundit, S. Luewan, Fetal ventricular shortening fraction in hydrops fetalis, Obstet. Gynecol. 117 (2011) 84–91.
[158] H.A. Christian, Drug treatment of cardiac decompensation, J. Am. Med. Assoc. 108 (1937) 44–46.
[159] J. Zhao, W. Luo, Y. Xu, J. Ling, L. Deng, Potential reproductive toxicity of multi-walled carbon nanotubes and their chronic exposure effects on the growth and development of Xenopus tropicalis, Sci. Total Environ. 766 (2021) 142652.
[160] H. Campbell, R. Handy, D. Sims, Shifts in a fish's resource holding power during a contact paired interaction: the influence of a copper-contaminated diet in rainbow trout, Physiol. Biochem. Zool. 78 (2005) 706–714.